MODELLING AND EXPERIMENTAL VALIDATION OF NEAR DRY EDM

A DISSERTATION

Submitted in partial fulfilment of the

requirements for the award of the degree

of

MASTER OF TECHNOLOGY

in

Mechanical Engineering

(With Specialization in Production and Industrial Systems Engineering)

By

TUSHAR JOSHI

(17540010)

DEPARTMENT OF MECHANICAL AND INDUSTRIAL ENGINEERING
INDIAN INSTITUTE OF TECHNOLOGY, ROORKEE
ROORKEE-247 667 (INDIA)
JUNE 2019

CANDIDATE'S DECLARATION

I hereby declare that the work carried out in this project report titled "**MODELLEING AND EXPERIMENTAL VALIDATION OF NEAR DRY EDM"** is presented in partial fulfilment of the requirement for the award of the degree of **Master of Technology** with specialization in **Production and Industrial Systems Engineering** submitted to the department of **Mechanical & Industrial Engineering, Indian Institute of Technology Roorkee, India**, under the supervision and guidance of **Dr. PRADEEP KUMAR**, Professor, MIED, IIT Roorkee, India, and **Dr. AKSHAY DVIVEDI,** Professor, MIED, IIT Roorkee, India.

I have not submitted the matter embodied in this report for the award of any other degree or diploma.

Date: Jun 2019 **TUSHAR JOSHI**

Place: Roorkee 17540010

CERTIFICATION

This is to certify that the above statement made by the candidate is correct to the best of my knowledge and belief.

Dr. Pradeep Kumar
Professor
M.I.E.D
IIT Roorkee
UK-247667, India

Dr. Akshay Dvivedi
Associate Professor
M.I.E.D
IIT Roorkee
UK-247667, India

ACKNOWLEDGEMENT

I wish to express my deep sense of gratitude and sincere thanks to my guides, **Dr. Pradeep Kumar,** Professor, Mechanical and Industrial Engineering department, IIT Roorkee, **Dr. Akshay Dvivedi**, associate professor, Mechanical and Industrial Engineering department, IIT Roorkee, for introducing me to this topic, being helpful and a great source of inspiration. I would like to thank them for providing me with an opportunity to work on this excellent and innovative field of research. Their keen interest and constant encouragement gave me the confidence to undertake the project work. I wish to thank them for their constant guidance and suggestions without which I could not have successfully completed this seminar.

I would like to thank **Dr. B.K. Gandhi**, HOD MIED, IIT Roorkee for his constant support during my study. I would like to thank Mr. Vineet Kumar and Mr. Ramveer Singh, Research Scholar, Mechanical and Industrial Engineering department for their valuable suggestions and fruitful discussions related to this work. I would also like to thank all the teaching and non-teaching staff members of the department who have contributed directly or indirectly in successful completion of my project work.

Date: Jun 2019

Place: Roorkee

TUSHAR JOSHI

M Tech, PISE

II year

Enrol. No. 17540010

Abstract

The Electrical Discharge Machining process is used widely for making tools, dies, deep hole drilling, metal disintegration machining and close loop manufacturing. Material removal in EDM takes place due to thermal erosion as a result of discrete repeated discharges that take place between the tool and the work piece. A dielectric fluid plays a significant role on the machining efficiency of Electric discharge machining (EDM). On the basis of number of phases involved in dielectric fluid EDM process can be categorized.

Two phase (liquid-air) dielectric medium is utilized in near-dry (EDM). It is an environmentally friendly process. In near dry EDM the dielectric medium is in the form of vapour or mist bubble. According to the research work done as of yet, flushing after machining depths more than 10mm has been one of the short comings of the process. Debris reattachment to tool causes side sparks leading to poor quality characteristics or outcomes of process like hole overcut.

The main objective of this study was to come out with solutions to enhance the flushing of IEG and thereby improve MRR, reduce hole overcut and study tool wear rate. For this purpose flow characteristics of bi-phase mixture in IEG and its vicinity was simulated using ANSYS fluent 19.0 where inlet conditions namely, air pressure and liquid flow rate were altered along with three different geometries of tool electrode. Results of simulation indicated that tool geometry with helical flutes was most effective for deep holes since it provided maximum velocity in IEG (392m/s) with velocity vectors pointing out of drilled holes, tool with peripheral slots was also effective with high pressure and high liquid flow rate.

Further experimental results pointed out that MRR was highest when tool with helical flutes were used, although hole over cut was minimum with tool having peripheral slots and it was concluded by ANOVA that tool geometry was of utmost importance to control MRR and TWR but had minimal effect on hole overcut while pressure is most influencing flow parameter to control hole overcut.

Keywords: Rotary tool near dry EDM, holes, material removal rate (MRR), Tool wear rate (TWR), overcut, ANSYS fluent Multiphysics 19.0, inter electrode gap (IEG)

CONTENTS

LIST OF FIGURES

LIST OF TABLES

CHAPTER 1

INTRODUCTION

Rapid industrial growth assisted with technological advancement witnessed the demand to machine and manufacture materials which provides higher strength to weight ratio, heat resilience and hard materials, encompassing there use in aerospace, nuclear and various other industries. The new era of manufacturing effectively uses unconventional sources of energy like electron or ions, light, sound, mechanical and chemical. Developments in the field of material science have led to production of metallic material, composites, ceramics etc. which has enhanced thermal, mechanical and electrical, thermos-electrical properties. Owing to these improved properties, manufacturing these material to final, ready to be used, product becomes a night mare and hence comes the requirement of machining processes that can effectively machine these difficult to materials. Non-traditional machining processes and in particular Electro-discharge machining is answer to all these problems. These processes are termed non-traditional in the sense that they do not employ the hitherto involved machining techniques i.e. they use other, already mentioned, forms of energy for machining instead of using direct physical contact between tool and work-piece. In post industrialization era these processes find unlimited expanse with respect to their usage. The problems faced in achieving complex shapes with precision and accuracy have been exquisitely handled using these and any other process has, by far, has remained un-parallel in terms of achieving outputs synonymous to them.

Electric discharge machining (EDM) is one of the most used non-traditional or advanced machining process. The only requisite for deploying EDM for machining is that the workpiece or material to be machined, should be conductive irrespective of its hardness of material or complexity of shapes required to be machined. The Electrical Discharge Machining process is used widely for making tools, dies, deep hole drilling, metal disintegration machining and close loop manufacturing**.** Material removal in EDM takes place due to thermal erosion as a result of discrete repeated discharges that take place between the tool and the work piece. Both the electrodes namely tool and workpiece needs to be submerged in the dielectric medium which maybe hydrocarbon oils, deionized water, glycerin etc. Use of hydrocarbon oils is most common in commercially available EDM. Amongst all positives there resides a huge disadvantage

associated with such hydrocarbon oils. The evaporation of these oils produce harmful fumes which are hazardous for both machine operator as well as they pollute environment. Low material removal rate (MRR), high tool wear rate, pollution and problem to operator viz-a-viz harmful fumes are the most common cons of using conventional EDM. In order to circumvent these drawbacks researchers, in past three decades, have come out with several variations such as use of gas as dielectric medium also known as dry EDM[1], use of two phase namely liquid and gas (pressurized) termed as near dry EDM (NDEDM)[2] and use of solid particle in liquid dielectric termed as powder mixed EDM (PMEDM)[3]

Amongst all variation used until now, NDEDM using rotation of tool has outlasted every other variation in terms of higher MRR, lower TWR, lower hole over cut etc. Primary concern of this study is to analyze the same i.e. Rotary tool near dry EDM.

1.1 Near Dry EDM

This variant of EDM was designed and developed by Tanimura et al.[2]. As already mentioned, NDEDM uses bi phase mixture as dielectric medium. A compressor is used to pressurize the gas which is there after mixed with liquid dielectric medium whose flow rate is regulated using a pump. When this liquid comes in contact with high pressure gas it gets atomized into very small particles termed as mist. This mist which is then passed through an annular electrode (tool) acts as the dielectric material in working area of inter-electrode gap. The idea behind using mist instead of gas alone is to reduce re-attachment of debris to tool electrode. The liquid particle cools and, in turn, solidify debris and there after the high pressure mist flushes it out of inter electrode gap before they re-attach to tool electrode. Pulse duration along with discharge current also plays an important role in surface integrity. The choice of gaseous phase and liquid phase also plays an important role in performance of near dry EDM. Gases capable of creating exothermic reactions that liberate more heat energy in IEG results in better MRR[4], is avoided. Prandtl number and dynamic viscosity is vital regarding the choice of liquid phase. Liquid which has higher value of both viscosity and prandtl no. yields more heat energy in IEG. Another endeavor made to expedite process efficacy is giving rotatory movement to tool and exploit centrifugal action of rotating tool to excavate the IEG which results in better surface finish.

1.1.1 Material Removal Mechanism

The exact mechanism of material removal in near dry EDM was still in veil till 2015 when dhakar et al. [5] visualized process with help of image processing and high speed imaging. Process begins with quasi-homogenous distribution (meshing) of fluid droplets or mist in inter electrode gap IEG as shown in Figure 1(a). This distribution takes in direction of current which bridges the gap between tool and workpiece (IEG). Due to difference in electric potential between tool electrode and workpiece electrode these mist droplets attains some charge depending upon the threshold limit (Figure 1b). These mist droplets which are now carrying charge accelerate which moving towards the work electrode and subsequently transfer there charge to work electrode and explodes on the surface of workpiece as shown in Figure 1(c).

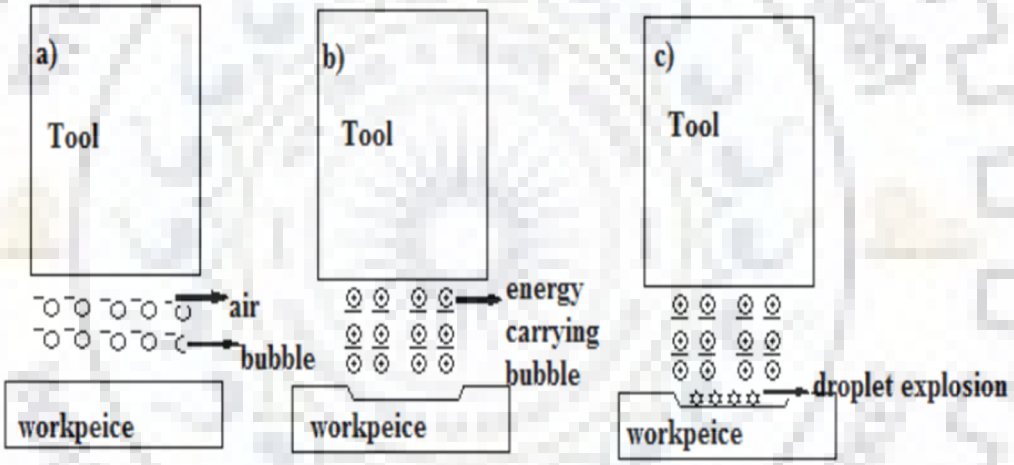

Figure 1 schematic representation of material removal in near dry EDM [5]

This distributed explosion results in series of discrete discharges in IEG. All these actions in tandem helps in flushing of removed material from IEG and higher order material removal from work area. The presence of liquids in IEG helps in cooling debris particles and solidify them before they attach to tool electrode. Fast and distributed sparking inside the inter electrode gap (IEG) leads to uniform erosion of material from work piece surface. Better surface finish of both tool surface and work surface provides more uniformity in pattern of sparking and hence uniform removal of material from work piece surface which is indispensable for good results in near dry EDM.

1.1.2 Dielectric Fluid

Dielectric fluid is, perhaps, one of the most distinguishing characteristic of near-dry EDM. Dielectric fluid is characterized by its dielectric strength which is defined as the maximum electric field strength that a medium can sustain without breakdown (without losing is insulating properties). NDEDM uses two phase or bi-phase fluid which is in general a mixture of highly pressurized gas and mass flow regulated liquid. Most common example of such dielectric used until now are mixture of deionized water and air, glycerine and air, kerosene and air, deionized and nitrogen further this list goes on and on. Initiating discharge and conveying spark in narrow region, cooling work electrode and tool electrode, flushing and cleaning of working area by carrying removed material or debris etc. are some of the important functions of dielectric fluid.

In the following experimental setup dielectric fluid used is mist consisting of deionized water and air which is regulated at different flow rate and pressure conditions.

1.1.3 Input Parameter of Near Dry EDM

Following section is a description of all input parameters that can be regulated r controlled in order to impact and enhance the performance of the process.

a) **Pulse-on time (T-on):** This parameter regulates the duration of time for which current is allowed to flow in every cycle. This parameter along with peak current in general regulates the amount of energy that is channelized in a particular cycle, which in turns decides the MRR and other output factors.
b) **Pulse-off time (T-off):** This parameter signifies the time duration between two consecutive sparks which is important as this duration of time give the time for flushing of IEG and also controls the stability of consecutive sparks.
c) **Arc gap:** This is the distance between tool electrode and workpiece electrode. It is controlled using servo system and is also known as spark gap.
d) **Discharge current (I):** This is peak or maximum current that is allowed to flow per cycle and is measured in current. Discharge current is directly proportional to MRR.

e) **Duty cycle (τ):** It is the ratio of pulse on time to total cycle time.

$$\tau = \frac{Ton}{Ton+Toff} \quad (1)$$

f) **Voltage (V):** It is the electric potential at power supply is given and directly controls the energy in each cycle and hence the MRR. It is one amongst the most important factor to control machining outputs. It is measured in Volts.

1.1.4 Output Parameters

The various output measures of the ultrasonic machining are:-

a) Material removal rate: It is defined as the amount of material removed from the workpiece per unit time. More the MRR, lesser will be the time required to complete the machining.

b) Tool wear rate: Tool wear directly affects the shape of drilled holes. Tool wear depends upon a number of factors such as work piece material, tool material, current, voltage, pulse-on time, flushing etc.

Tool wear rate is measured by reduction in the weight of tool divided by the machining time and density of tool material.

c) Surface roughness: It is one of the most important parameter to measure the quality of the drilled. Surface roughness mainly depends upon many factors as current, pulse-on time, voltage, flow rate of dielectric, inlet pressure etc.

d) Taper and Overcut: Taper is defined as the difference between the final dimensions of holes and the tool diameter because, some of the debris particles get trapped between the tool and the workpiece and cause unwanted side arching. Overcut is defined as the difference between the inlet diameter and exit diameter of the holes. Overcut is due to the fact that as the depth of cut increases, the flow of the debris between the tool and the workpiece gets hampered and hence the exit diameter is generally smaller than the inlet diameter.

1.4 Organization of Dissertation

The dissertation is organized in six different chapters. Details of each chapter are as follow:

- Chapter 1 contains a brief introduction of rotary tool near dry EDM along with explanation of basic process mechanism.
- Chapter 2 is all about literature review of available text regarding simulation and modelling of various parameter of the process.
- Chapter 3 explains a basic model of tool and workpiece, where initial and boundary condition are described which were taken into account. This chapter also accounts for simulation results and brief discussion
- Charter 4 discusses the experimental procedures that were undergone and changes in tool geometry. In the later part experimental results are presented with brief discussion of results.
- Chapter 5 is devoted to validate the results of simulation with our experimentation results and also compares the results with existing literature.
- Chapter 6 is dedicated to conclude all the observations that were made in due course of study.

CHAPTER 2

LITERATURE REVIEW

The most promising and qualitatively exquisite process amongst non-conventional machining process for machining difficult to shape materials like high speed steel HSS, Inconel and machinist nightmare i.e. titanium etc. This process is extensively deployed for fabricating dies, molds etc. Amongst all positives there is still much room for improvement to enhance the efficacy of already mentioned process. Rotary tool near dry electric discharge machining (RT-NDEDM) is, by and large, a comprehensive solution for all negatives in EDM. The detailed review regarding studies moving around RT-NDEDM is presented below.

Tanimura et al [2] for the very first time in 1989 derived and eventually developed a new variation in EDM by using two phases, namely gas(air) and liquid(water), as dielectric medium where they flushed the mist at high pressure through annular or tubular electrode. Further they observed improved stable spark and also very less sticking of debris to tool because of effective flushing via high pressure stream of mist. One of the worst cons, poor odor of vaporized liquid dielectric was by and large eliminated.

Dhakar et al [5] investigated the use of mixture of high viscosity fluid glycerine and air for analysing individual effect of distinct parameters through RSM. It was found out that material removal rate (MRR) increased significantly with rise in all input parameters also a combination of parameters were analysed to set optimum combination which revealed that glycerine mist outclassed water mist in all response parameters i.e. MRR, HOC, taper and in terms of recast layer thickness.

Puthumana et al [6] investigated the performance of rotary tool near dry EDM using slotted tool and reported that use of peripheral slots on tool helps in flushing of melted debris from working zone more efficiently and hence deposition of debris at depths more than 10 mm is reduced and eventually MRR improves remarkably. DOE was implemented using a L16 matrix which optimized the machining parameter and revealed that a higher value of current (18 A) coupled with higher input pressure (.25 MPa) gave maximum MRR (1.497mm^3/min) and also debris accumulation to tool was reduced. Further experimentation were done using 2, 3, 4 and 5 slots

and it was reported that tools with slots less than 4 were less effective, current and voltage along with duty factor also played important role in tandem with slots on electrode.

Fujiki et al [7] developed a meticulous CFD model to study the effects of lead angle (which is the angle between "vector projected over the plane which is created between normal to work surface and direction of feed" and normal to the plane) and tilt angle (which is the angle between "vector projected over the plane which is created between normal to work surface and direction of cross feed) on the volume fraction of various components of mist in working area which explained the importance of volume fraction of air as well kerosene on MRR, surface roughness.

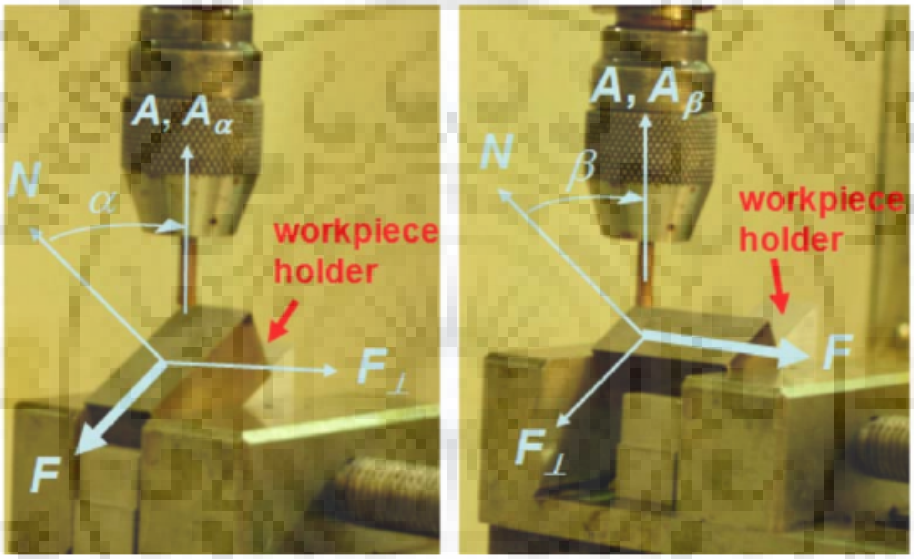

Figure 1 Edited picture with various planes and lead angle 'α' and tilt angle 'β' [7]

Simulation represented that a lower negative value of lead angle provided higher fraction of kerosene in working area which may result in higher MRR and later this was experimentally validated. The experimental results showed that MRR was directly proportional to flow rate of dielectric which was another finding of simulation. This study also focused on impact of choice of mesh size over simulation results, where very-very fine mesh was taken at critical areas to improve accuracy of results while, coarse mesh at place with less importance to reduce calculation time.

Zhang et al [8] studied what is now known as scaling effect or the impact of tool size i.e. tool length and diameter on surface integrity of machined surface and notice the impact of stray capacitance while machining with lower values of energies which was, hitherto, ignored but its impact was found commendable while micro machining at low energy. Scaling effect was found

to have feeble influences when the discharge gap was high in micro machining with deionized water as dielectric.

Wang et al [9] was the first in line to study the effect of helical tool coupled with rotary movement of tool electrode to create a controlled centrifugal ambience near tool which provided upward thrust along with devoted passage (or flute) for debris to escape the working area. A CFX model was developed and velocity vectors were traced in the vicinity of tool and it was observed that velocity vectors tend to pass through helical flutes on tool periphery. This simulation was experimentally validated where it was found that with increase of tool rotation there was increase in MRR, which plunged after a certain maximum value of tool rotation (3000 rpm).

Bhaumik et al [10] investigated the effect of tool material on the surface integrity (micro cracks density, radial overcut and surface roughness). The experimentation was conducted by setting similar machining input parameters for copper, aluminium and brass tool and comparisons were made in terms of parameters mentioned earlier. It was observed that copper tool outclassed both brass and aluminium tool by giving best surface finish even at lower peak current (10A). Copper was followed by aluminium while brass tool yielded worst surface finish. Recast layer was bare minimum in copper as compared to that of brass and aluminium.

Oezkaya et al [11] investigated the need of micro cooling channels in tool which helps to carry away heat in case of work piece with lower thermal conductivity. CFD was utilized to understand the rate of heat transfer, accountability of flow near flank faces as well as dead zones and thus tool life dependency on various factors was analyzed. This simulation was further experimentally validated which concurred the simulation results by revealing that higher values of mass flux provided no edge, regarding tool life, over tools having small coolant channels. Yet some difference, although small, with respect to deposition near tool flank surfaces were observed.

Gholipoor et al [12] investigated the effect of magnetic field in tandem with existing setup of near dry EDM, akin to use of centrifugal effect of rotating tool to clean debris machining area here magnetic force was used to do the same and the experimental observations revealed that near dry EDM with magnetic field outperformed conventional near dry EDM in flushing working area hence provided better MRR also surfacing integrity was also better which is another attribute of better flushing.

Tao et al [13] developed a CFD model to simulate micro near dry EDM process where the simulation was divided in to two steps namely plasma heating phase and bubble collapsing phase which simulated interaction of more than one phase using VOF modelling in ANSYS fluent. Here implicit properties were chosen for mist which was a combination or average of properties of both component phases. This simulation predicted the crater depth with very less error and revealed that smaller crater and lower pressure conditions are connected to lower pulse energy at the time of discharge. All these giving of simulations were validated experimentally.

Mullya et al [14] modelled a 2D simulation project where accretion behaviour of debris particle was simulated in micro drilling EDM process and flow behaviour of debris particle in machining was studied by assuming the debris particles as spherical balls at nanoscale. This model revealed the trajectory of debris particle and also their accretion rate. The results of simulation were further experimentally validated. The experiments as well as simulation showed that orientation of tool rotation decided the debris trajectory, also when small particles of debris accumulated to form relatively large particles the accretion rate increased. Higher tool speed also avoided accretion of debris along tool wall.

Xie et al [15] developed a fluid flow numerical simulation model to understand impacts of ultrasonic vibration on EDM and debris motion behaviour and its mechanism due to these vibrations. The study revealed that the debris accumulation away from the periphery are larger and hence holes at centre are lager as compared to periphery. Debris flow was observed better at exit when ultrasonic vibration were used at higher frequency.

Fujiki et al [16] investigated ive-axis near dry EDM to study the tool path planning to check the mist leakage while milling over a curved surface. The study was to optimize the positions of tool and its orientation in order to minimize the lead angle as also decipher maximum and minimum path of tool travel to check the leakage of mist. Experimentation validation was conducted and it was noticed that plunge method yielded best MRR for engaging method. Crowning of tool tip due to debris tool wear it became difficult to identify minimum path travel responsible for mist leakage.

Bai et al [17] investigated the effect of power mixed near dry EDM (which is broadly EDM using three phase dielectric) and revealed enhanced output parameters like higher MRR with low energy input. This improvement was basically attributed to enlarged discharge gap, which is facilitated by easier breakdown of dielectric medium because of improved electric strength. Density of energy

is greater because of augmentation of motion resistance force of medium that surrounded the plasma channel and hence force that accounts for material removal is enhanced.

Yadav et [18] investigate the effect of peak current, tool rotation speed flushing pressure and liquid flow rate on the process economics using glycerine and air as dielectric and machined to a depth more than 23 mm which is very high when it comes to near dry EDM. The experimentation concluded optimized factor to achieve depths more than 20 mm in NDEDM drilling process.

2.1 Research Gaps

After the introduction of highly pressurized multi-phase dielectric medium through tubular electrode, many improvisations have already been made in order to enhance the performance the machining outputs regarding its implementations at industrial level. Yet material removal after certain depth has succumbed to keep pace with the rate as it happens at shallow depth in drilling or milling processes. After the review of literature some key findings regarding improvisations are, use of dielectrics having higher value of viscosity, providing rotation motion to tool, assisting the process using external magnetic field as well as ultrasonic vibrations at various frequencies, changing the orientation of tool to give tilt and lead angle to adjust the mist leakage while working over curved surfaces. Nature of material of tool and its dimensions have also been altered to improve the machining characteristics. Although provision for peripheral slots and helical flutes in tool have found there use limited to dry and wet EDM respectively. Hence there exist an opportunity to exploit these subtle, yet important, changes to tool geometry in order to analyze their impact on machining outputs.

2.2 Objectives of Present Work

Based on the literature review and the gap areas identified, the objectives of the present work are formulated as follows:

1. In ND-EDM the rate of material removal gradually falls with increasing depths, so aim of this work is to maintain the pace of material removal even while machining deeps holes, which will ultimately improve the net material removal rate of the process.
2. Ineffective flushing of IEG leads to reattachment of debris to side walls of tools resulting in side arching and subsequently increasing hole over cut. This study aims to minimize side

arching and hence reduce hole overcut so that desired dimensions of machined surface are obtained with utmost accuracy.

2.3 Scope of Present Work

Amongst multiple dimensions on which RT-NE-EDM can be worked upon to enhance the quality characteristics of output, the scope of this study is limited to bring in geometrical changes in the tool to enhance flushing of IEG. The scope of this work is described in the following points:

1. To simulate the flow of bi phase mixture with conventional tubular tool, tool with four peripheral slots and tool with helical flutes at different levels of gas pressure and liquid flow rate, thus find the effect of shape of tool along with air pressure and flow rate on velocity magnitude and velocity vector direction. Hand in hand simulate the mixture fraction at areas of tool workpiece interaction, to check whether mist leakage in proposed tool alters the fraction of liquid and come out with best possible tool shape and flow parameters.
2. Further conducting experimentation by varying input parameters that were considered in simulation and optimize parameters in order to fulfill the objective of research.
3. Finding a correlation between simulation results and experimental observation.

CHAPTER 3

SIMULATION OF BI-PHASE MIXTURE ACROSS THE PASSAGE FOR MIST EXIT AND MAIN DICHARGE REGION

3.1 Problem Definition

Analysis of fluid flow in the region where tool in inside the workpiece at depth 10mm where accumulation of debris takes place, to examine the velocity vectors of mist and volume fraction of deionized water. Both of these results are analyzed for conventional tool, tool with rectangular slot and tool with helical flutes with pre-defined pitch.

3.2 Methodology Adopted

For simulating the flow of the fluid and volume fraction of deionized water in gap region between tool and work piece, ANSYS fluent *Multiphysics-19* software is used. ANSYS fluent Multiphysics is a simulation tool for electrical, mechanical, fluid flow, and chemical applications. It is a software platform, which uses numerical methods, for modelling and simulating various physics-based problems. With ANSYS fluent Multiphysics software, we can also perform Multiphysics simulations like simulation which includes more than one phase at a time.

3.3 Workflow for Modelling Fluid Flow and Volume Fraction

There are certain steps for modelling any of the geometry in ANSYS fluent Multiphysics software. These steps are as follows:

1. Define the geometry by using modelling tools or by importing the file.
2. Select the material of the geometry e.g. copper, aluminium etc.
3. Select the appropriate fluid properties and chose a suitable physics interface e.g. defining phases, fluid flow interface etc.
4. Define initial conditions and boundary conditions.
5. Define the mesh.
6. Compute the results and finally, we can visualize the results.

3.4 Assumption for Simulation

Since it is next to impossible to exactly translate the practical experiment in computer based technology, it is necessary to make suitable assumptions to attain results near to reality. Following are the assumptions made for simulating the process.

1. Deionized water was assumed to be incompressible since pressure in working domain is not very high.
2. Density of air and deionized water was assumed to remain constant and were assigned the value of room temperature and are temperature independent.
3. All the boundaries that were touching work piece remain stationary.
4. All the boundaries that were touching tool were rotating with velocity same as tool.
5. Entrance effects for fluid flow were ignored.
6. The distance (gap) between tool and workpiece were assumed to be constant.

3.5 CAD Model Used for Defining Various Regions

Following section describes the assembled as well as busted view of geometry which was analysed using ANSYS fluent.

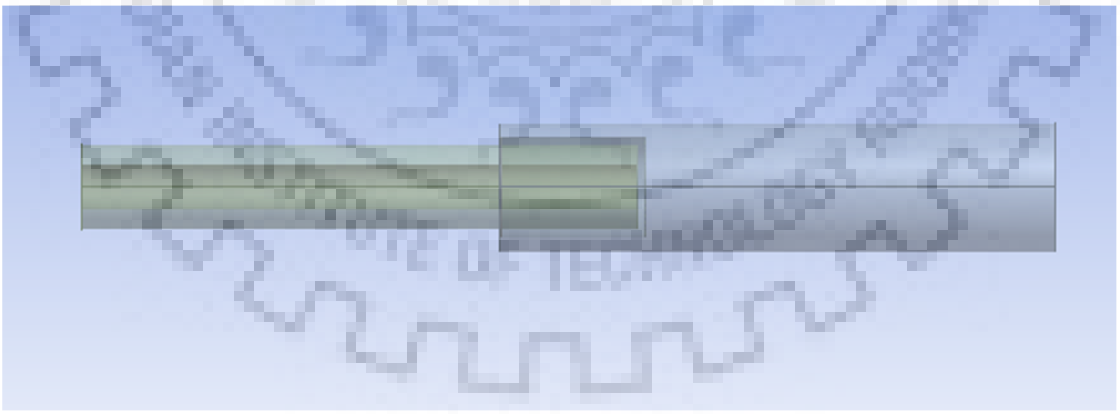

Figure 2: Side view of tool engulfed inside tool at depth 10mm

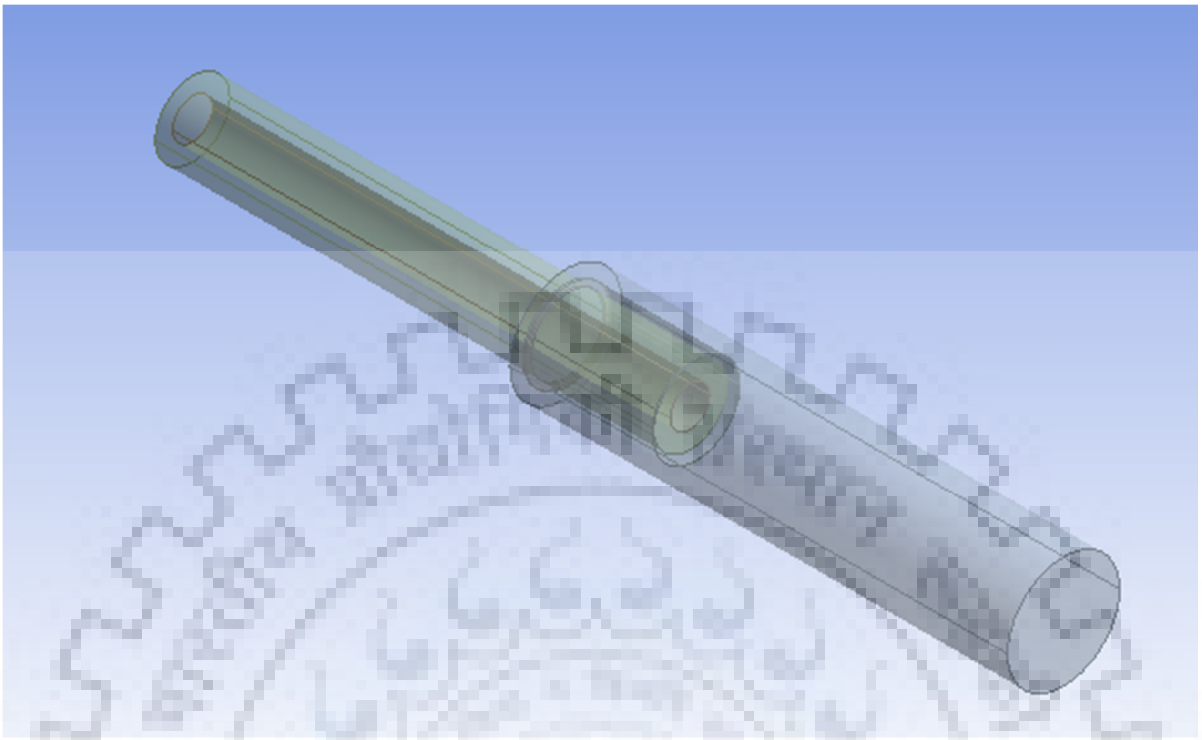

Figure 3 Isometric view of tool engulfed inside workpiece at depth 10 mm

Figure 2 and 3 represent the side view and isometric view of conventional tool which is engulfed up to 10 mm depth inside the cylindrical cavity in work piece with IEG equal to 30µm which is estimated using previous experimental measurement.

Following section represents the busted view of all important regions with regard to modelling. Yellow colored portion in the following figures is used to specify each object individually.

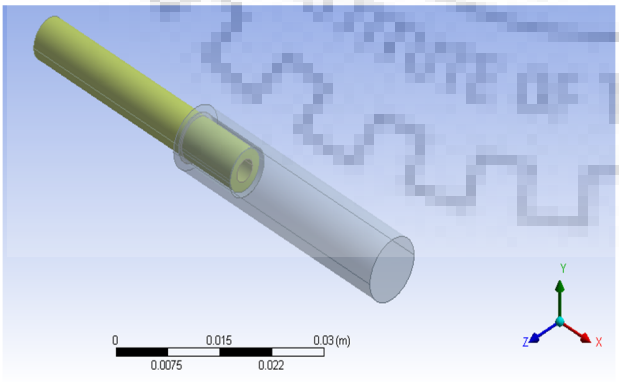

Figure 4 Tool

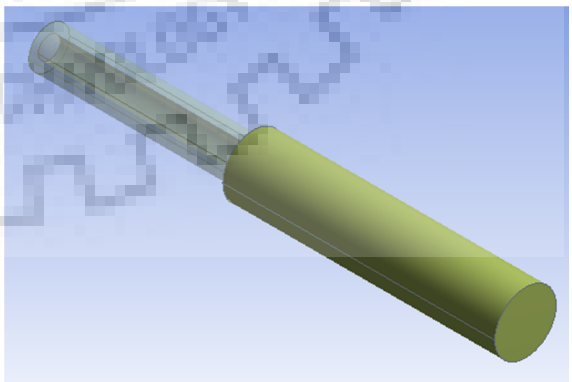

Figure 5 Work piece

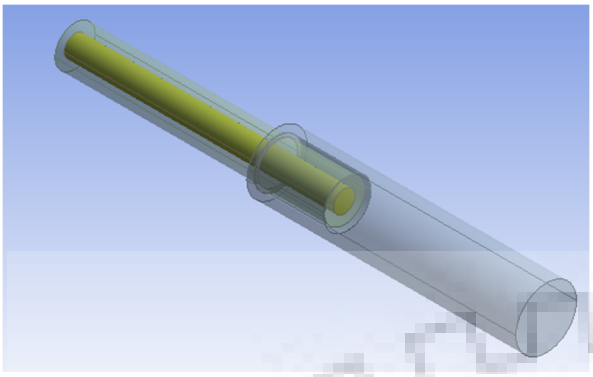

Figure 6 Inlet passage of mist

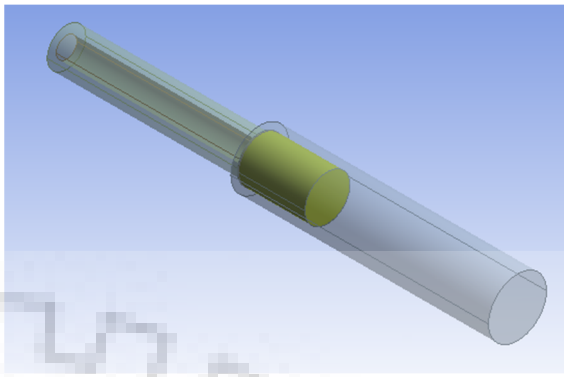

Figure 7 Main discharge region

Figure 4, 5, 6 and 7 represent every important section namely tool, work piece, inlet passage of mist, main discharge reason and cylindrical cavity.

Following the CAD assemblies of slotted as well as helical tool inside cavity.

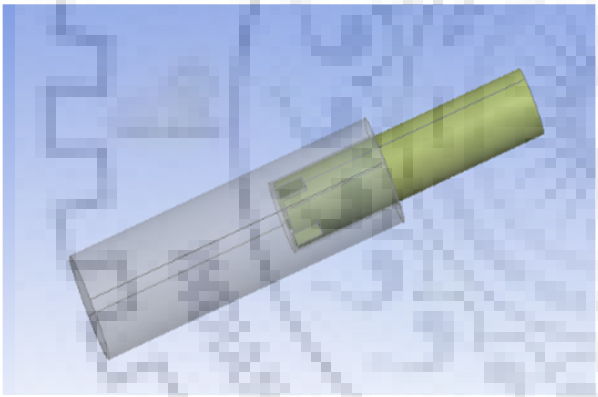

Figure 8 Tool with peripheral slot

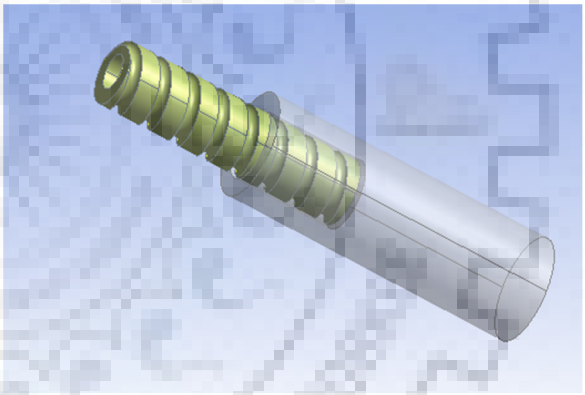

Figure 9 Tool with helical flutes

Figure 8 represent annular tool with external radius 3 mm and internal radius 1.63 mm having 4 equi-spaced square slots of dimension 1mm ×1mm. Figure 9 represents tool of same internal and external radius but peripheral slots of dimension .57mm×1.63mm which are helically carved over tool surface with pitch 3.21mm.

3.6 Design for Simulation

The simulation is designed as follows:

1. Material of tool or solid body walls were set as copper.
2. Model used was laminar flow solver.
3. Modelling of mist or mixture flow was volume of fluid (VOF) model with implicit scheme.
4. Physical parameter of
   i) Deionized water : density = 995kg/m^3, dynamic viscosity =.00089 Pa. s
   ii) Air : density= 1.225 kg/m^3, dynamic viscosity= 18.1µPa. s
5. The inlet for mist was set as mass flow boundary condition.
6. Outlet boundaries were set at ambient conditions.
7. Rotation speed of tool was taken as 1000 rpm.
8. Mesh size plays an important role in terms of accuracy and simulation time finer the mesh size accurate are the result coarser the mesh size more is the inaccuracy, yet very fine mesh size increases the time taken for calculations. Hence physics controlled finer-mesh was used in the given simulation.

3.7 Simulation Results and Discussion

After running calculation for 1000 iterations the results converged for all cases of analysis. Following were the results drawn after analysis. The results observed are presented in two sections. First section shows the velocity vectors and magnitude of velocity of mist particles at two region namely IEG and tool region where tool is inside the cavity or say passage for exit of mist and debris from cavity created. Second section show the volume fraction of deionized water in both regions mentioned earlier.

To understand the simulation results better, Figure 10 clearly defines both the region. The region marked with black color is IEG and the region shown in orange color is the region for passage of mist from cavity while carrying debris. Region mentioned in green color is beyond the interest of simulation results. White color arrows show the direction for mist and debris to exit from work area.

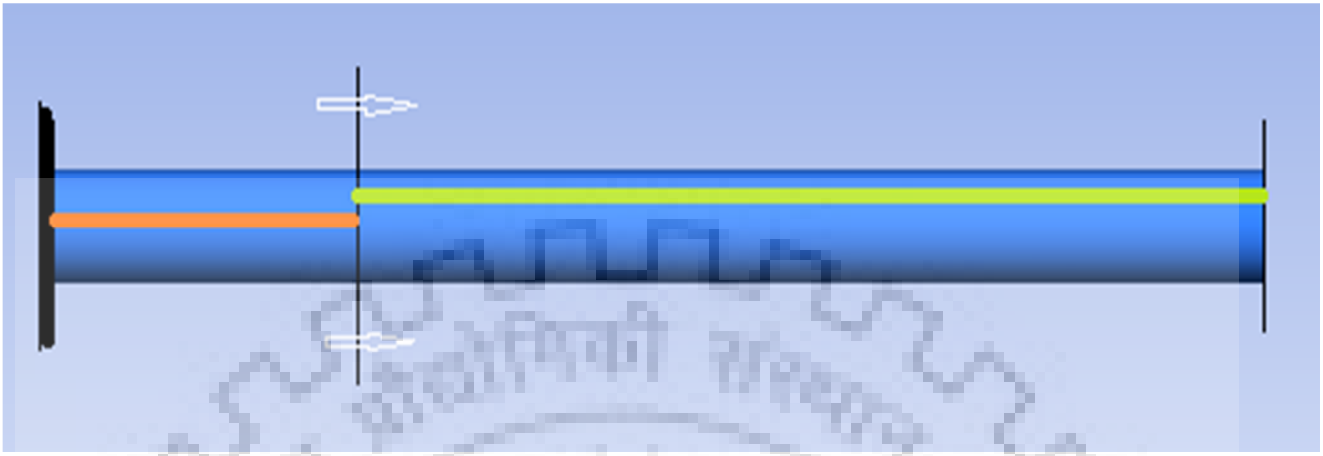

Figure 10 schematic representing various areas to understand simulation results

3.7.1 Simulation Results for Velocity Vector and Magnitude of Velocity

1. Conventional Cylindrical Annular Tool

The tool is given clockwise rotation when seen from right end of image

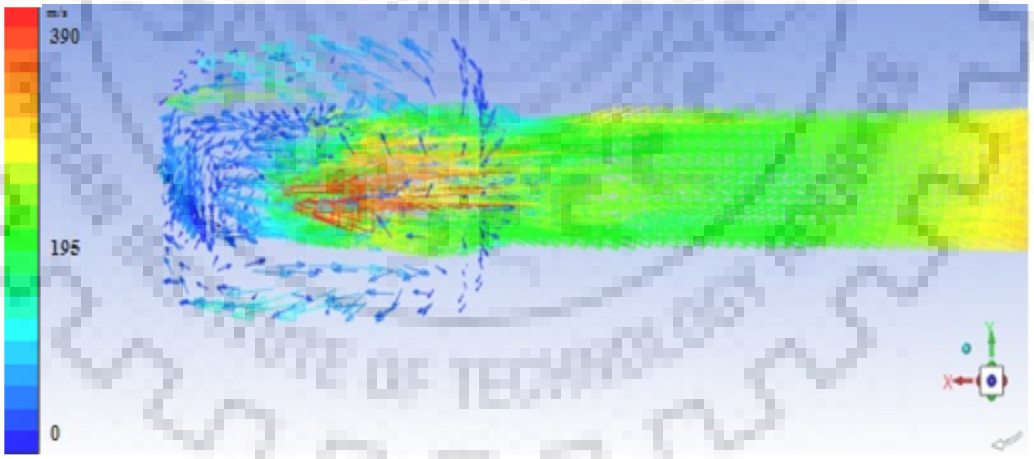

Figure 11 Velocity vector in fluid flow zone

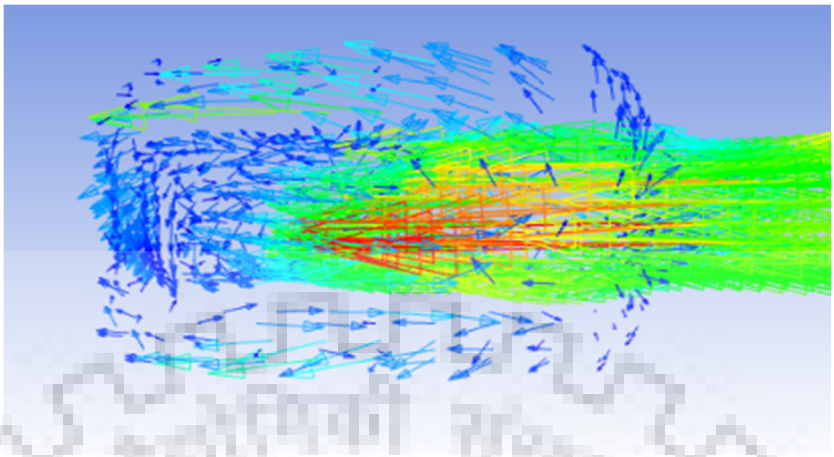

Figure 12 Magnified image of velocity vector in main discharge region

Minimum mist velocity = 12m/s (at IEG)

Maximum mist velocity = 248m/s (at entry of mist inside workpiece)

It is clearly evident from the velocity vectors in Figure 11 that after a certain depth, 10 mm in this simulation, velocity of mist in IEG reduces to a very low value due to which it becomes almost incompetent to carry debris from main discharge region. Another takeaway from this simulation is that at the location where mist moves out from workpiece a whirl is created where velocity vectors are hardly facing out which means a reverse flow condition is created which is yet another evidence of ineffective flushing of machining area. Further coupled effects of mist volume fractions are discussed in next section.

2. Tool with Peripheral Slots

The tool is given clockwise rotation when seen from right end of image.

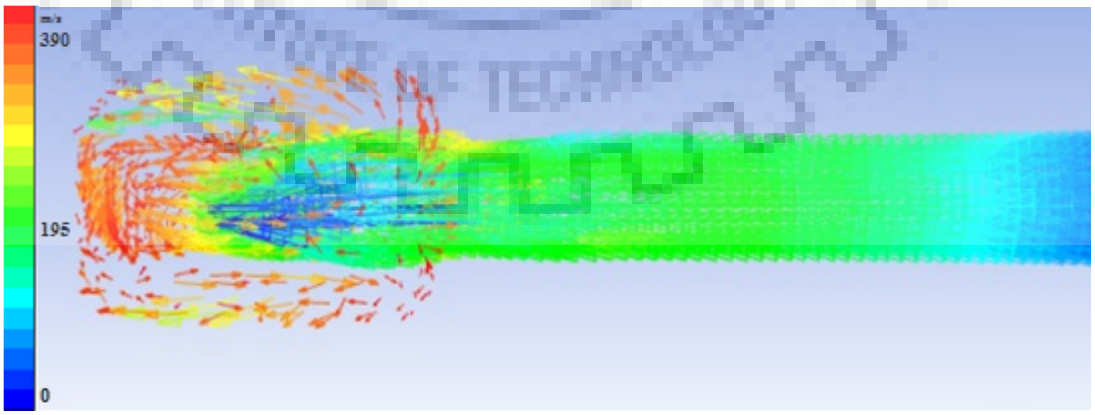

Figure 13 Velocity vector in fluid flow zone

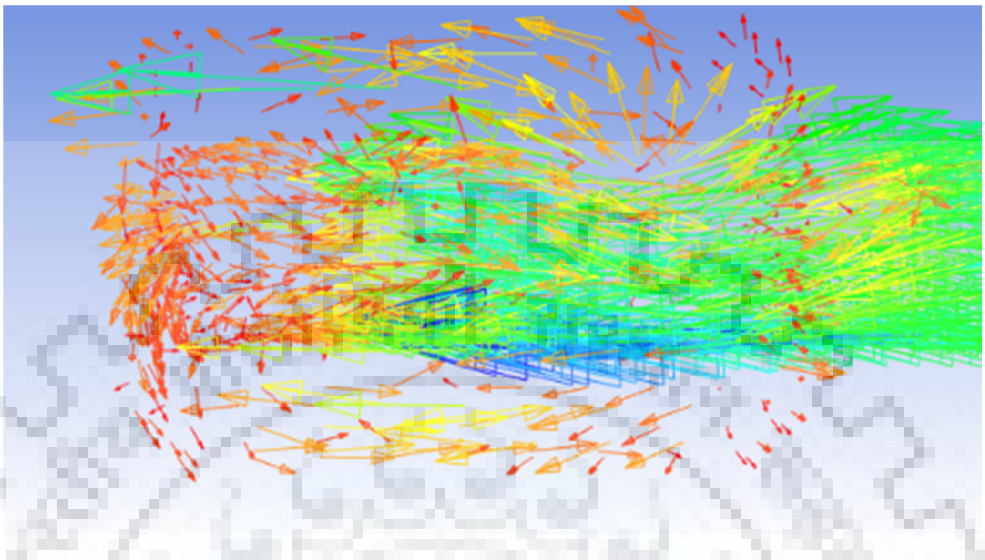

Figure 14 Magnified image of velocity vector in main discharge region

Minimum mist velocity = 48 m/s (at peripheral slots opening)

Maximum mist velocity =362m/s (at IEG and exit of mist from workpiece)

Observing the Figure 13 of simulation with slotted tool it can be seen that velocity at IEG, MDR and mist exit is higher as compared to conventional tool, this is a result of non-stagnant condition created in work area because of extra passage for mist which evidently reduces blockage. By observing velocity vector, some reverse flow condition can still be observed before the mist exit region, which is however less as compared to previous case. Thus we can conclude that although high velocity regions are observed in IEG yet reverse flow conditions that are created are inhibiting the flushing in full-fledged manner and hence there is still room for improvement.

3. Tool with Helical Flutes

The tool is given clockwise rotation when seen from right end of image

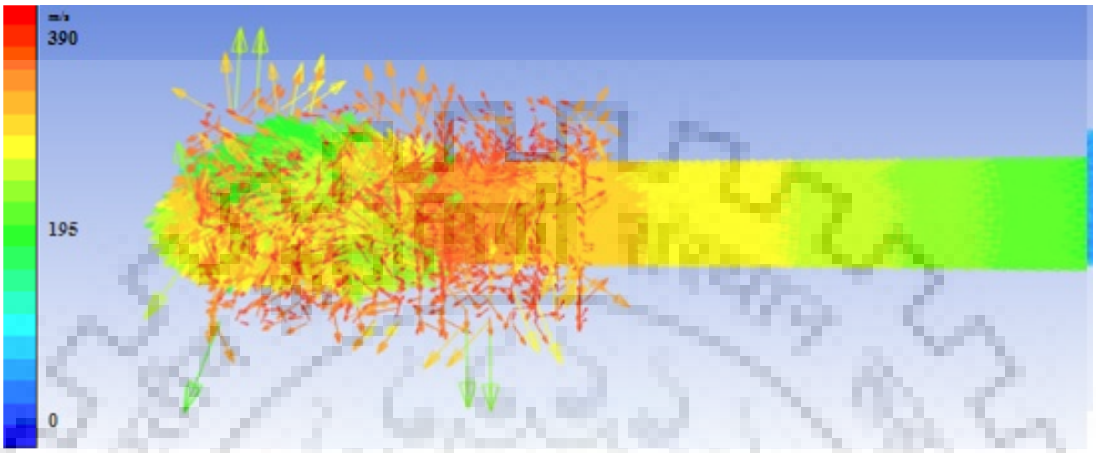

Figure 15 Velocity vector in fluid flow zone

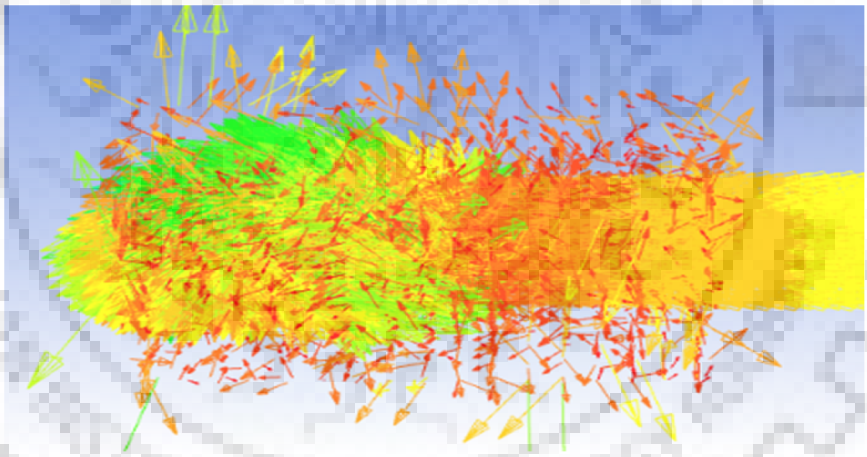

Figure 16 Magnified image of velocity vector in main discharge region

Minimum mist velocity= 44m/s

Maximum mist velocity=384m/s

From Figure 15, one key takeaway is that although there is not much change in magnitude of velocity yet there is uniformity, by and large, in distribution of o magnitude of velocity and hence reverse flow condition at exit is fairly low. Thus we can staunchly claim that this case exemplifies better flushing not just at IEG but also at the mist exit region. But

yet no claims can be made for machining efficiency unless we are very sure of mist composition of at main discharge region. Although this flow simulation assures us that flushing is best in case of helical tool, since it has guided path for mist till mist exit region, followed by slotted tool and conventional tool appeared to be worst of all these.

CHAPTER 4

EXPERIMENTATION WORK

4.1 Rotary Tool Near Dry EDM Setup

A commercial EMS 5030 die sinking EDM was used for experimentation. A dielectric mixing unit was utilized in near-dry EDM for inter-mixing of fluid and air. This unit was de-signed and fabricated in Advance manufacturing process (AMP) laboratory at IIT Roorkee, India. Figure 17 is the schematic representation of setup which was used for experimentation, which constituted a compressor to pressurize the air, power supply unit, servo system, mixing unit, a pump to regulate flow rate of liquid dielectric, electric motor to provide rotary motion to tool.[18]

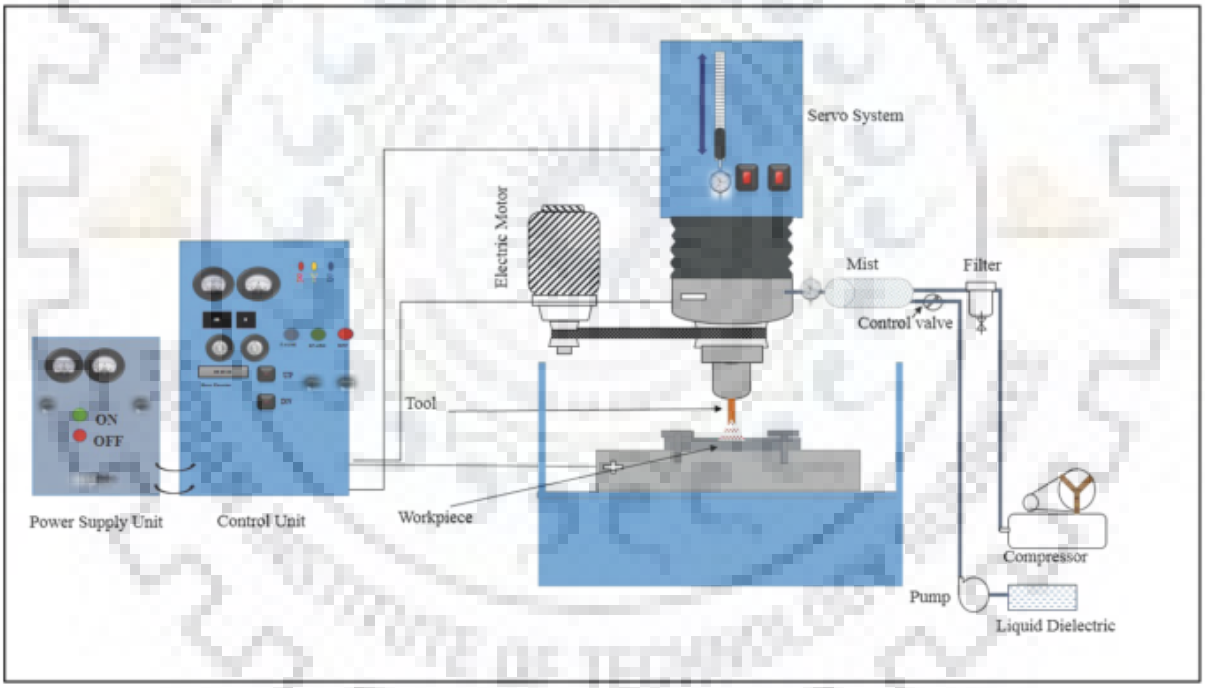

Figure 17 Schematic representation of rotary tool near dry EDM [18]

4.2 Selection of Workpiece

High speed steel was selected for the experiments. HSS is a conductor which is the primary requirement for its use in ND-EDM. It has high working strength and is difficult to machine. It is

resistant to corrosion thus it avoids much corrosion losses due to presence of water and ambient contact[19]

4.3 Selection of Tool Material

A study was conducted by **Bhaumik et al** [10] which compared the effect of tool material on the performance of EDM process. The study used the tool made of copper, aluminum and brass which concluded that copper tool outclasses both other tool material in all terms related to machining outcomes. Further copper has high thermal conductivity and high specific heat constants to prevent the heating of tool. The main concern with this study required tool modification. The tool material is required to undergo various machining modification and copper is easily Machinable and hence required geometry could be easily carved on it. Copper is conducting in nature which primary requirement for tool in ND-EDM.

4.3.1 Preparation of Tool

After having decided the material of tool as copper next imminent step was preparation of tool. Dimensions of tool used for experimentation purpose and modelling are same.
Procedure followed to prepare tool is as follow:

1. A solid copper rod of external diameter 8mm was taken and equal pieces of length 55.1mm (55 mm tool length and .1mm for machining tolerances) were cut out of it.
2. A through hole (concentric with copper rod) of diameter 4 mm was drilled using vertical drill machine with suitable dill bit.

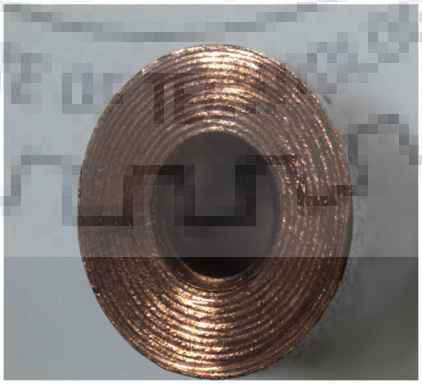

Figure 18 Back view of toll after drilling through hole

3. Now this piece was turned to diameter 6mm for length of 25mm from one end. The prepared piece of tool until now is the conventional tool for RT-NDEDM as show in figure 3.3

Figure 19 Image of conventional RT-NDEDM tool

4. Next step was to prepare “type 1” tool, which has peripheral slots of depth 2 mm and width 1.5 mm in it (according to the drawing made for it). Figure 20 (a & b) shows the side and top view of the tool after peripheral slots.

(a) (b)

Figure 20(a) Side view (b) top view of tool with four peripheral slots respectively

5. On the conventional tool (as shown in Figure 19), were machined to prepare “type 3” tool. Figure 21 (a & b) show side and top view of tool

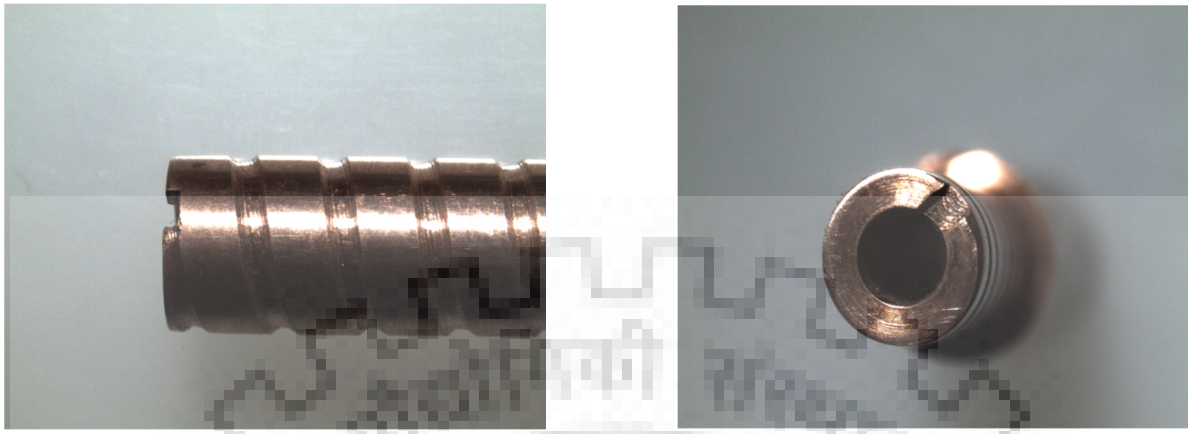

(a) (b)

Figure 21 (a) Side view (b) Top view of tool with single start helical flutes

Similar process was repeated to prepare 3 tool of each type and all of these tools were fine polished using emery paper to reduce unevenness or surface roughness so that a good interaction between tool and workpiece is initiated. Following table constitutes the mass of each tool which will be later required to calculate tool wear rate.

Table 1 List of all tools with their weight before machining

Tool name		Tool initial weight(in grams)
type 1 tool 1		15.9811
type 1 tool 2		16.0103
type 1 tool 3		15.8601
type 2 tool 1		15.7091
type2 tool 2		15.7763
type 3 tool 3		15.6992
type 3 tool 1		15.5854
type 3 tool 2		15.43215
type 3 tool 3		15.3372

4.4 Selection of Process Parameters

Before considering the Taguchi design of experiments, a detailed evaluation of various process parameters was carried out to find out the key parameters that can affect the quality of the holes

being drilled on high speed steel using RT-ND-EDM. To evaluate these parameters Ishikawa's cause and effect diagram was developed (Figure 22).

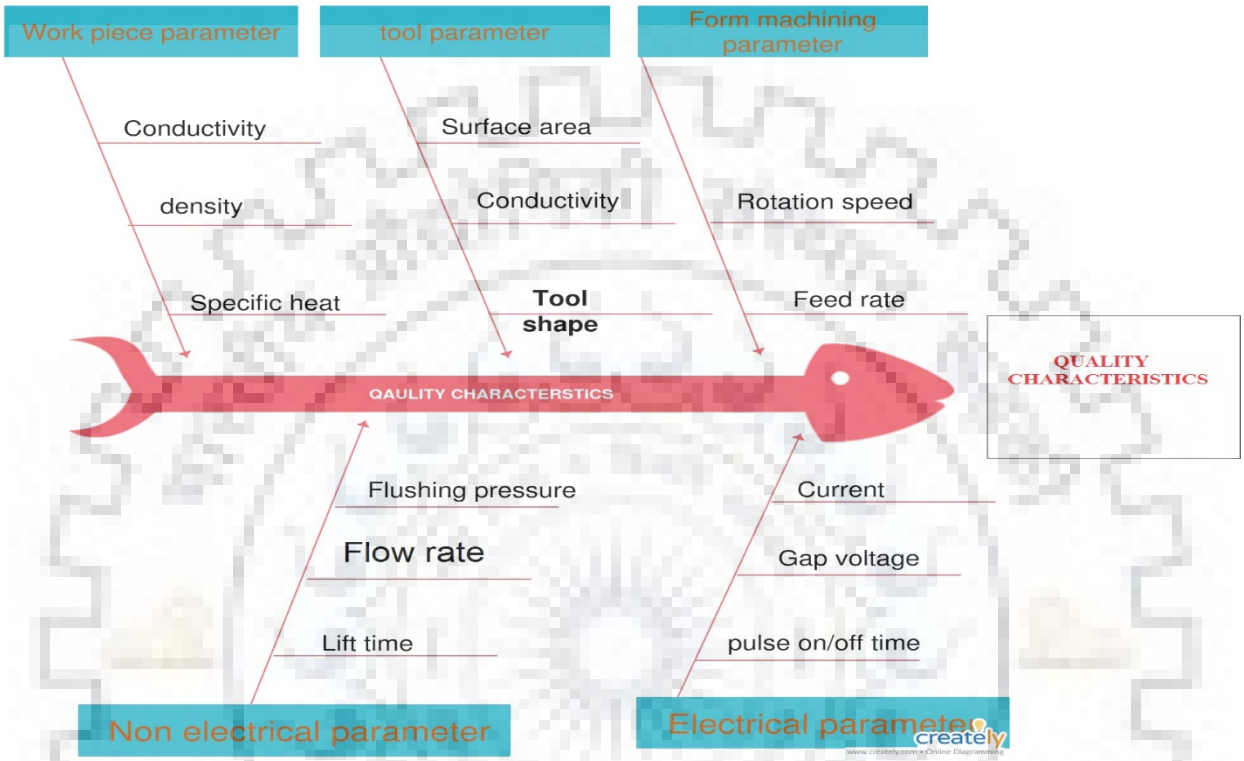

Figure 22 Ishikawa cause and effect diagram

By this cause and effect diagram, the following key parameters are chosen to study their effect on the quality of the drilled holes:

1. Flushing pressure
2. Tool shape (modified tool periphery)
3. Flow rate of dielectric

Noise factors (factors which can't be controlled by the operator) are not taken into consideration because, including these parameters may complex the experimental work.

4.5 Input Parameters/Control Factors

In the present study out of the large no of process parameters, effect of the following parameters was studied on machining of the holes:

1. Flushing pressure
2. Tool shape (modified tool periphery)
3. Flow rate of dielectric

4.6 Output Parameters

Following are the quality characteristics which were investigated in our present study:

1. Material removal rate (MRR)
2. Hole over-cut (HOC)
3. Tool wear rate (TWR)

4.7 Constant Parameters

There are some of the process parameters which were kept constant during the whole experimentation work. These are:

1. Current : 10A
2. Ton: 240µs
3. Tool rotation speed: 1000 RPM
4. Workpiece material : HSS
5. Polarity : straight (tool negative)
6. Lift : 2
7. Dielectric medium: deionized water and air
8. Tool material : copper

4.8 Design of Experiments

For our present study, we have used Taguchi design of experiment (DOE) method to examine the effect of above stated input process parameters on the output parameters. By using taguchi DOE method, various parameters can be optimized simultaneously and it also tells us about the percentage contribution of each parameter by using the ANOVA analysis. By using Taguchi DOE

approach, much more quantitative information can be extracted by performing very less number of experimental trials [20].

In Taguchi DOE method, an orthogonal array (OA) is used to examine the effect of a large number of variables with a very few experimental runs and the data is analyzed very easily and efficiently by using signal-to-noise (S/N) ratio. Using this method, the research and experimental costs can be reduced by simultaneously studying a large number of parameters [16].

Taguchi uses signal-to-noise (S/N) ratios as response variables. Signal-to-Noise (S/N) Ratio is a single response which makes a tradeoff between setting the mean to a desirable level while keeping the variance low. If the noise is less, we will get a better signal. So, we always try to maximize the S/N Ratio. There are three types of S/N ratios:

- Smaller is Better,
- Target is Best,
- Larger is Better.
- The selection of the most suitable type of S/N ratio depends upon type of the quality characteristic to be optimized. For example, we always try to minimize the surface roughness. So, we will use smaller the better S/N ratio. After calculating the S/N ratio for each of the response variable, analysis of variance (ANOVA) is carried out to find out the percentage contribution of each input variable on the output.
- The S/N ratio for the 'Smaller-the-better' type of response is used for Taper, Overcut, Corner Radius and Average Surface Roughness and is computed as:

$$(S/N)_{LB} = -10 \log \left[\frac{1}{R} \sum_{i=1}^{R} y_i^2 \right] \quad (2)$$

Where, R is the number of all data points and y_i is the value of the i^{th} data point [20].

4.8.1 Selection of an Orthogonal Array

In our present work, three process parameters were studied each at three levels. These levels are chosen based on the past researches. Based on this, L_9 OA was selected for the experimental

analysis as shown in table 2. The symbol L_9 signifies that a total of 9 experimental runs have to be carried out to complete our study.

Table 2 List of process parameters at different levels

Parameter-designation	Process parameter	Level 1	Level 2	Level 3
A	Pressure(in psi)	25	50	75
B	Liquid flow rate(in ml/min)	3	6	9
C	Type of tool	Type 1 (tubular tool)	Type 2 (tool with peripheral slots)	Type 3 (tool with helical flutes)

4.8.2 Experiments Using Taguchi Design:

Design Summary:

Taguchi Array	L9(3^3)
Factors:	3
Runs:	9

Minitab19 software was used to carry out the various calculations of the present design of experiments. Table 3 shows the values of the response variables at various combinations of the input parameters:

Table 3 Taguchi DOE using orthogonal array

Run	Pressure (in psi)	Flow rate (ml/min)	Tool type	MRR (mm^3/min)	TWR (mm^3/min)	Overcut (in mm)
1	25	3	1	1.02	0.0015	0.2961
2	25	6	2	1.26	0.0121	0.2633
3	25	9	3	2.26	0.0164	0.2589
4	50	3	2	1.33	0.0125	0.3316
5	50	6	3	2.14	0.0156	0.3615
6	50	9	1	1.08	0.0121	0.2811
7	75	3	3	2.15	0.0161	0.2733
8	75	6	1	1.63	0.0142	0.3422
9	75	9	2	2.07	0.0151	0.2788

Material removal rate was recorded my measuring the weight of workpiece after successive runs and their difference gave the value of material removed, time was recorded for this period of machining and hence MRR was found out.

Overcut was measured by using the Stereo-microscope at 10X resolution of the drilled holes.

4.9 Results and Discussion

4.9.1 Analysis of Material Removal Rate (MRR):

Following section describes the observations made regarding MRR at different input conditions. The later part of this section discusses the observations and there pattern of variation with distinct input conditions.

- As the pressure was increased from 25 psi to 50 psi there was a slight increase in MRR. While MRR increased to great extent when the pressure was increased to 75 psi.
- As the flow rate was increased from 3mm^3/min to 9mm^3/min, near about linear increase in MRR was observed.
- As we use type 2 tool there is drastic increase in MRR as compared to conventional tool which further increased when we used type 3 tool. The results were far better for tool with helical flutes, while peripheral slots became nearly ineffective at these depths and hence MRR gradually reduced relative to tool 3.

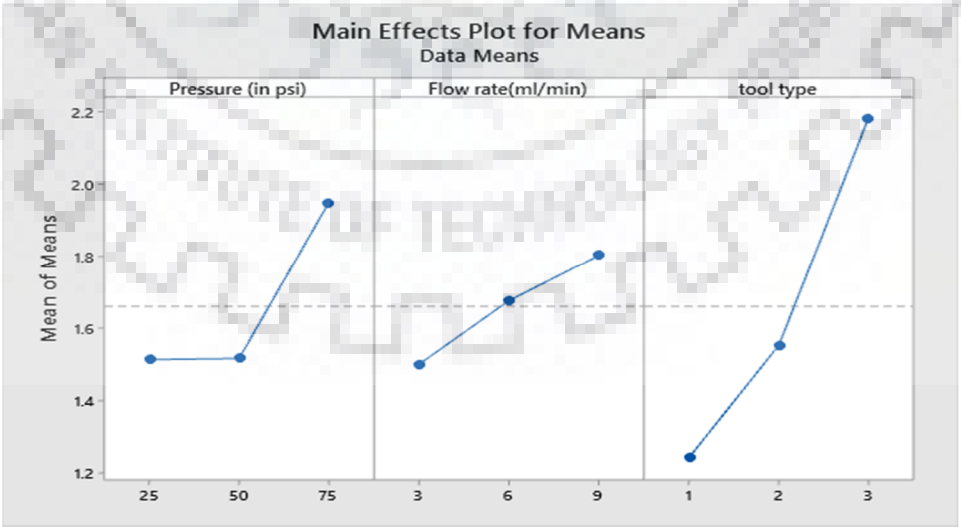

Figure 23 MRR at different levels of input parameters

From Figure 24 it is clear that highest value of S/N ratio was obtained at level 3 of gas pressure, level 3 of flow rate and level 3 of tool type. Hence, the optimum parameter setting for obtaining maximum MRR were **A3-B3-C3**. At this setting, the optimum value of MRR was given by [(1.95+1.8033+2.1833)/3] = 1.9788 mm^3/min.

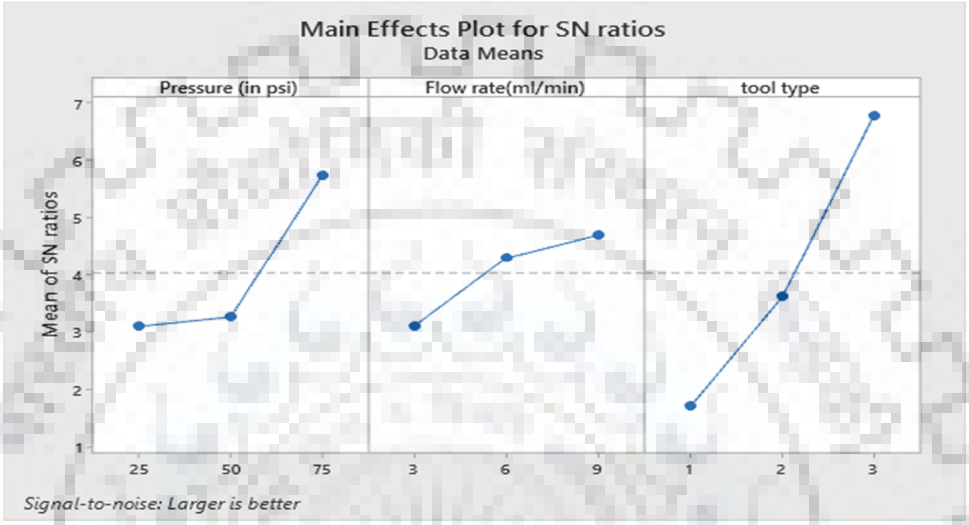

Figure 24 S/N ratios (MRR) at different levels of input parameters

From the ANOVA for SN ratios of MRR (Table 4), it was concluded that, type of tool has highest contribution 68.34%, followed by air pressure 18.79% and lastly liquid flow rate 6.91%.

Table 4: Analysis of Variance for SN ratios (MRR)

Source	Source	DOF	Seq. SS	Adj. SS	Adj. MS	F	%contribution(C)
Pressure (in psi)	A	2	.3785	.3785	.18932	3.15	18.79
Flow rate(ml/min)	B	2	.1393	.1393	.06963	1.16	6.91
tool type	C	2	1.3766	1.3766	.68830	11.47	68.34
Error	Residual Error	2	.1201	.1201	.06003		5.96
Total	Total	8	2.0144				

#DOF=degree of freedom, MS=SS/DOF, #SS=sum of squares

According to the observation recorded, tool shape is the most critical input. Among the three shape of tool that were used for experimentation, MRR with tubular tool was minimum and use helical tool resulted in maximum MRR. This is because of the guided path for debris exit in form of helical flute. Debris glided over the tool surface in that case and IEG gap was less contaminated resulting in stable sparking and hence material removal rate improved. While machining with tool having peripheral slot, it was observed that material removal at the beginning was very rapid but as the depth increased the space available, for debris exit, in form of slot became insufficient for debris removal. Although at high pressure (75psi) MRR recovered its pace to some extent and its value increased even with type 2 tool. The key takeaway from this discussion is that for drilling deep holes type 3 tool is most effective.

4.9.3 Analysis of Tool Wear Rate (TWR)

Following section describes the observations made regarding TWR at different input conditions. The later part of this section discusses the observations and there pattern of variation with distinct input conditions.

- As the air pressure and liquid flow rate were increased, there was evident increase in tool wear rate (TWR).
- Another similar observation follows, as the TWR is maximum in helical tool followed by tool with four slots and conventional tubular tool.

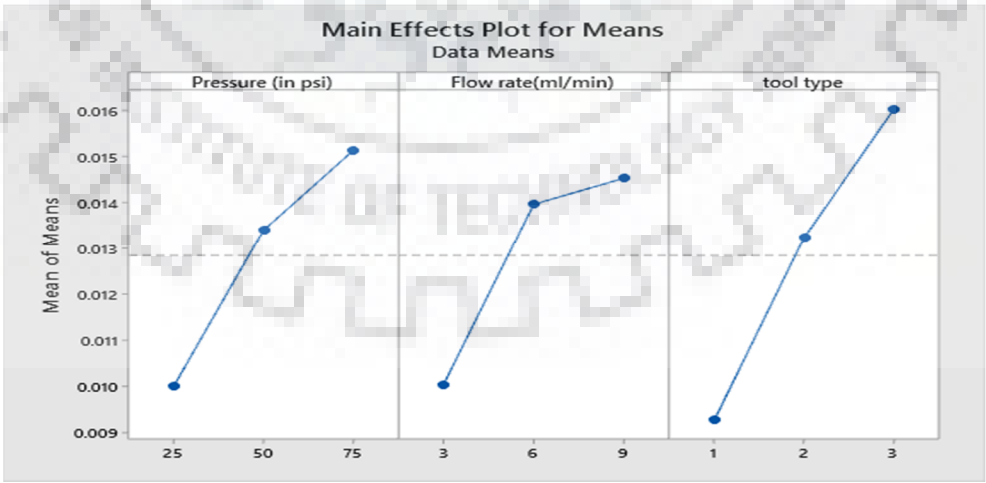

Figure 25 TWR at different levels of input parameters

From Figure 26 it is clear that highest value of S/N ratio was obtained at level 1 of pressure, level 1 of flow rate and level 1 of tool type. Hence, the optimum parameter setting for obtaining minimum Overcut were **A1-B1-C1**. At this setting, the optimum value of TWR was given by [(.01513+.01453+.01603)/3=.0152311]

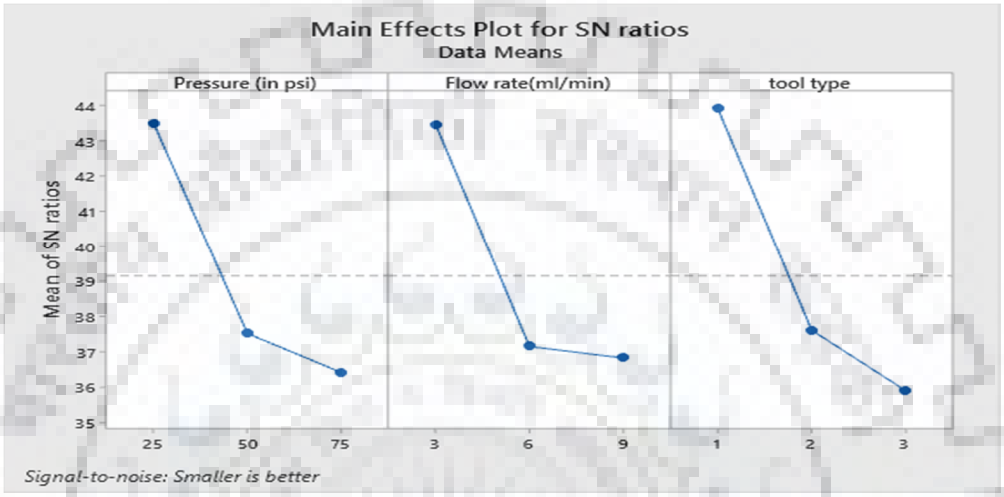

Figure 26 S/N ratios (TWR) at different levels of input parameter

From the ANOVA for SN ratios of TWR (Table 5), it was concluded that tool (C) has the major effect on TWR (63.24%) followed by pressure (19.59%) and liquid flow rate (12.81%) and each of the input parameters has the significant effect on the TWR.

Table 5: Analysis of Variance for SN ratios (MRR)

Source	DF	Seq SS	Contribution	Adj SS	Adj MS	F-Value
Pressure (in psi)	2	0.000024	19.59%	0.000024	0.000012	4.49
Flow rate(ml/min)	2	0.000016	12.81%	0.000016	0.000008	2.94
tool type	2	0.000078	63.24%	0.000078	0.000039	14.51
Error	2	0.000005	4.36%	0.000005	0.000003	
Total	8	0.000123	100.00%			

#DOF=degree of freedom, MS=SS/DOF, #SS=sum of squares

As we know that tool wear can be measured in form difference in weight of tool before machining an after machining. Usually there is some erosion of material from tool during machining process

which reduces its weight but some debris gets attached to tool periphery and hence there is gain of weight. Thus lower tool wear is indicative of more debris reattachment to tool. According to the observation, tool type is most influencing factor for TWR but air pressure is also an important factor.

The maximum tool wear was obtained for tool type 3 with high pressure. This indicates that while the debris passes over the flutes, the high air pressure effectively ensures that contact between tool and debris is removed before the debris reattaches over it. But in case with low air pressure with helical tool, the debris passing over tool surface reattaches on its surface before leaving the contact resulting in lower TWR.

4.9.4 Analysis of Overcut:

Following section describes the observations made regarding MRR at different input conditions. The later part of this section discusses the observations and there pattern of variation with distinct input conditions.

- There was increase in diameter over cut as pressure was increased from 25psi to 50psi. Value of overcut was reduced when the value of pressure was increased to 75 psi.
- Over cut was minimum with slotted tool followed by tool with helical flutes. While the hole over cut reached its maximum value when conventional tubular tool is used. As shown in Figure 3.11

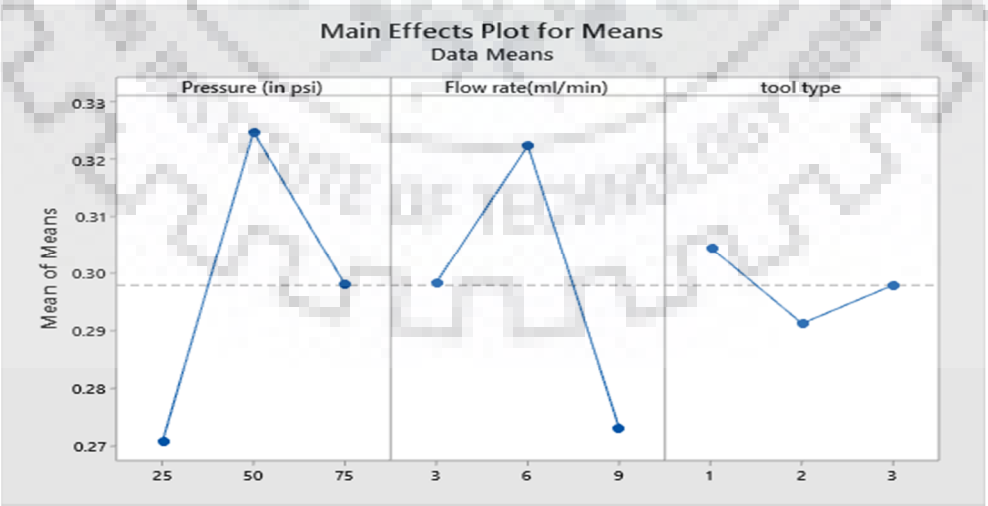

Figure 27 Diametrical overcut at different levels of input parameters

From figure 28 it is clear that highest value of S/N ratio was obtained at level 1 of pressure, level 3 of flow rate and level 2 of tool type. Hence, the optimum parameter setting for obtaining minimum Overcut was **A1-B3-C2**. At this setting, the optimum value of TWR was given by [(.2707+.2729+.2912)/3=.2782]

From the ANOVA for SN ratios of diameter overcut (Table 6), it is concluded that air pressure (A) has the major effect on hole overcut(44.07%) followed by flow rate(25.80%) and liquid flow rate (6.52%) and each of the input parameters has the significant effect on the hole overcut.

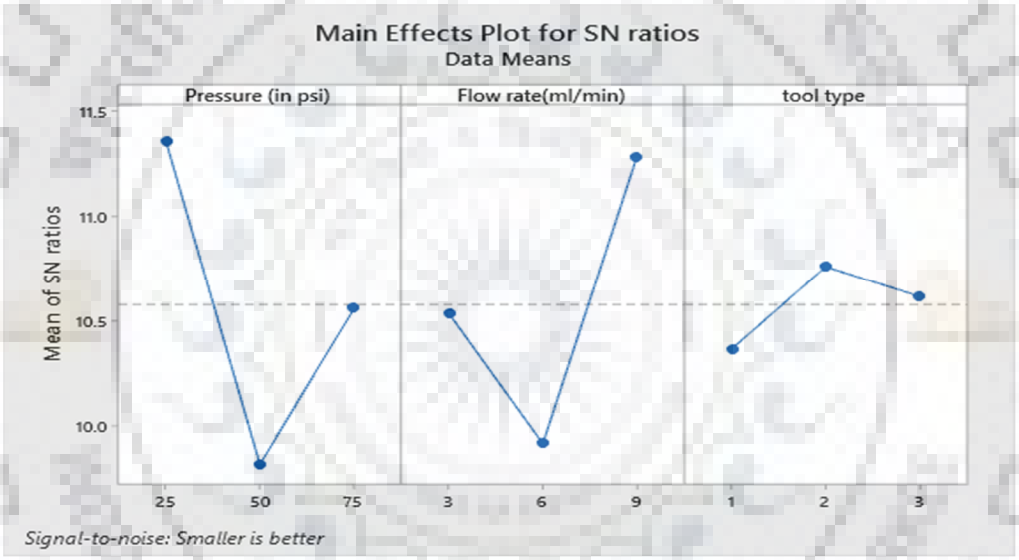

Figure 28 S/N ratios (diameter overcut) at different levels of input parameters

Table 6: Analysis of Variance for SN ratios (HOC)

Source	DF	Seq SS	Contribution	Adj SS	Adj MS	F-Value
Pressure (in psi)	2	0.004047	44.07%	0.004047	0.002023	1.87
Flow rate(ml/min)	2	0.002369	25.80%	0.002369	0.001184	1.09
tool type	2	0.000598	6.52%	0.000598	0.000299	0.28
Error	2	0.002168	23.61%	0.002168	0.001084	
Total	8	0.009182	100.00%			

#DOF=degree of freedom, MS=SS/DOF, #SS=sum of squares

According to the observations, hole over cut is maximum with conventional tool followed by helical tool and is minimum with tool having peripheral slots. According to over pervious discussion the minimum overcut should have been with tool type 3 it is not so. The main reason behind this is, as the debris glides over the helical flute at lower pressure conditions some debris collects over flutes and there are chances of side sparking resulting in unnecessary material removal due to more interaction time and hence higher over cut was seen. While such side sparking is at miniscule level for type 2 tool.

Air pressure is the most contributing factor regarding hole overcut. As the air pressure was increased from 20 psi to 50 psi there was increase in hole overcut this was because more interaction time increased side spark between the side surface of the copper tool and workpiece, resulting in higher overcut. When the pressure was further increased to 75 psi, the whole overcut reduces, this was because at pressure above 50 psi improved debris flushing from inter electrode gap, resulted in effective sparks between tool electrode and workpiece. Similar trend is observed with flow rate of liquid.

4.10 Conclusions

In the present study, we investigated the effect of air pressure, liquid flow rate and type of tool on, MRR, TWR and diametrical overcut of the micro-channels being machined on HSS using Rotatory tool near dry EDM. The following conclusions were made based on outcomes of the experiments:

1. For MRR, the highest value of S/N ratio will be obtained at level 3 of gas pressure, level 3 of flow rate and level 3 of tool type. At this setting, the optimum value of MRR is given by [(1.95+1.8033+2.1833)/3] = 1.9788 mm^3/min.
2. For TWR, the highest value of S/N ratio will be obtained at level 1 of pressure, level 1 of flow rate and level 1 of tool type. At this setting, the optimum value of TWR is given by [(.01513+.01453+.01603)/3]=.0152311mm^3/min.
3. For hole over cut, the highest value of S/N ratio will be obtained at level 1 of pressure, level 3 of flow rate and level 2 of tool type. At this setting, the optimum value of TWR is given by [(.2707+.2729+.2912)/3] = .2782mm.
4. From the ANOVA for SN ratios of MRR, it is concluded that, type of tool has highest contribution 68.34%, followed by air pressure 18.79% and lastly liquid flow rate 6.91%.

5. From the ANOVA for SN ratios of TWR (Table 5), it is concluded that tool (C) has the major effect on TWR (63.24%) followed by pressure (19.59%) and liquid flow rate (12.81%) and each of the input parameters has the significant effect on the TWR.
6. From the ANOVA for SN ratios of diameter overcut, it is concluded that air pressure (A) has the major effect on hole overcut(44.07%) followed by flow rate(25.80%) and liquid flow rate (6.52%) and each of the input parameters has the significant effect on the hole overcut.

CHAPTER 5

VALIDATION

The aim of this study was to model the flow of bi phase mixture in main discharge region of RT-ND-EDM and find out the velocity pattern, in term of magnitude and direction, at IEG and its vicinity. Next step was to conduct experiment by varying exactly the same parameters that were varied while simulating the same process. But the final and most important step of this study was to find a correlation between the experimental output characteristics like MRR, TWR etc. and simulation outputs i.e. velocity patterns. Following section validates the proposition made in assumptions.

Table 7 describes the experimental parameter that were chosen for experimentation. Simulation data was also collected for the similar setting of input parameters.

Table 7 List of parameter for experimentation and simulation

Run	Pressure (in psi)	Flow rate (ml/min)	Tool type
1	25	3	1
2	25	6	2
3	25	9	3
4	50	3	2
5	50	6	3
6	50	9	1
7	75	3	3
8	75	6	1
9	75	9	2

In the simulation results maximum velocity for all the cases were recorded at IEG which gradually decreased towards the mist exit region. Table 8 shows the magnitude of velocity vector and experimental output namely MRR, TWR and overcut. It clearly evident that MRR increases as the maximum magnitude of velocity increases corresponding to geometry of tool, air pressure and liquid flow rate. TWR varies inversely with velocity in almost all the cases.

Table 8 Simulation outputs and experimentation outputs

Run	velocity of mist (in m/s)	MRR (mm^3/min)	TWR (mm^3/min)	Overcut (In mm)
1	212	1.02	0.0015	0.2961
2	262	1.26	0.0121	0.2633
3	392	2.26	0.0164	0.2589
4	291	1.33	0.0125	0.3316
5	384	2.14	0.0156	0.3615
6	246	1.08	0.0121	0.2811
7	385	2.15	0.0161	0.2733
8	326	1.63	0.0142	0.3422
9	356	2.07	0.0151	0.2788

Figure 29 shows the variation of MRR with maximum magnitude of velocity of mist in IEG. The pattern of variation clearly represents that as the velocity of mist in IEG increases there is increase in value of MRR

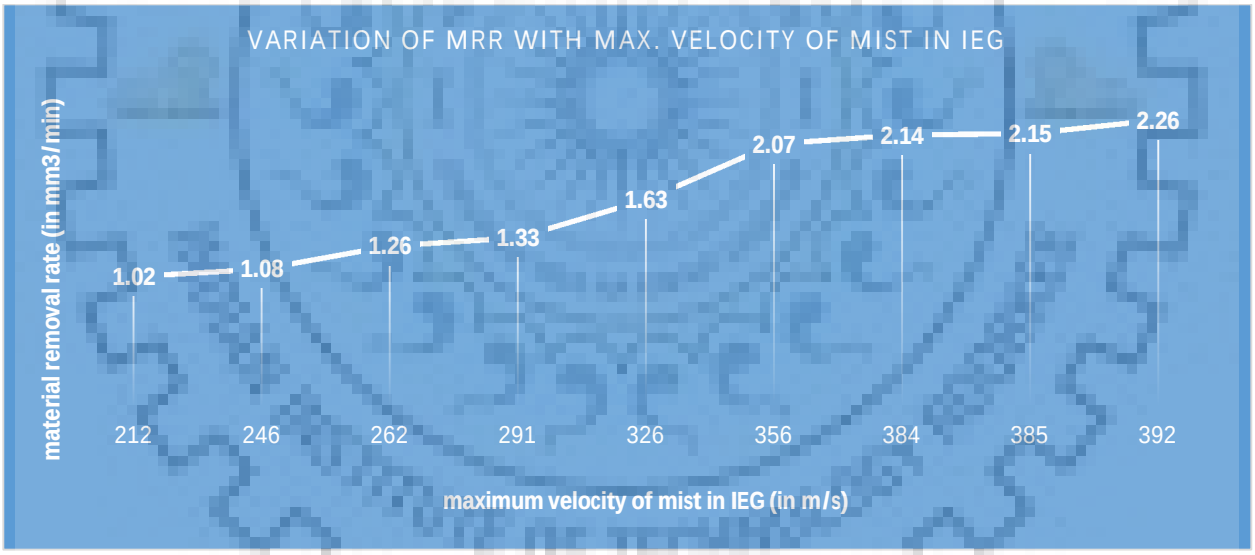

Figure 29 Variation of MRR with magnitude of velocity of mist in IEG

The velocity is dependent on many parameters like inlet air pressure, liquid flow rate and tool geometry. Maximum values of velocity of mist in IEG were obtained when type 3 tool geometry (384, 385, 392 m/s) was used. From our simulation results it was concluded that as the mist velocity increases, its debris carrying tendency increases and there is better flushing of IEG, thus MRR must increase. Trend shown in Figure 29 validates the proposition made in simulation. According

to experimentation and modelling done by fizuki et al [7] similar trends were revealed where changes in lead angle and tilt angle, increased the mist velocity in main discharge region which in turn improved the MRR. Use of tool with helical tool by wang et al [7] concluded similar motion of dielectric from flutes which enhanced debris flushing and experimentation revealed better MRR.

Figure 30 shows the variation of TWR with maximum velocity of mist in IEG. It shows that there is increase in TWR as the velocity of mist in IEG increases.

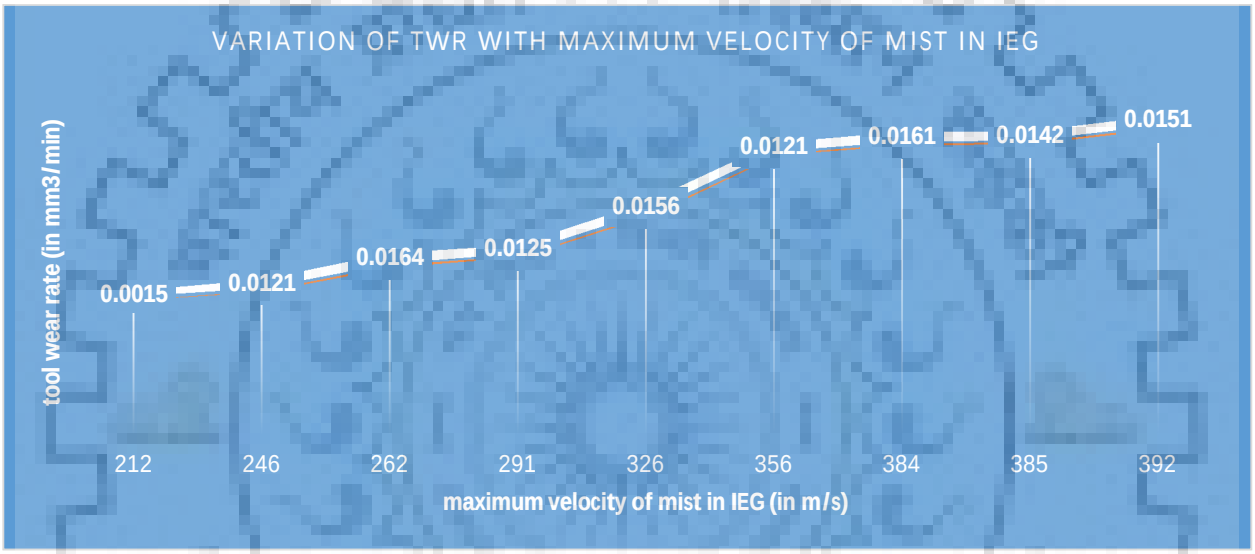

Figure 30 Variation of TWR with maximum velocity of mist in IEG

It was observed in simulation that with increase in magnitude of velocity of mist, velocity vectors pointed outwards (more violently) and were seen moving towards the mist exit region, also the formation of swirl conditions due to reverse pressure conditions also minimized. While in cases with lower velocity magnitude of mist it was observed that vectors were hitting the tool wall which is indicative of the fact that interaction time between tool and debris will increases thus there can be debris reattachment to tool which in turn will increase tool weight and show lower values of TWR. Tao et [] reported same finding , where it was reported that TWR increases as the interaction time reduces between tool wall, debris and hole inner walls decreases. The results of simulations exactly concurs with the experimental observations where there is increase in tool wear rate with cases of simulation corresponding to higher velocity.

Having validated our observations of flow simulations (velocity magnitude and vectors) with experimental data. Next task at hand was to observe the simulation results using VOF model to obtain fractions of each phase of dielectric in the main discharge with input conditions as optimized parameters given by ANOVA and understand the physics of process. Following sections show the simulation results o VOF model with input characteristic mentioned along with simulation

5.1 Correlation of VOF model of simulation with experimentation

From results of ANOVA it was seen that optimized value of MRR was obtained at pressure 75psi, liquid flow rate 9ml/min, helical tool type. Figure 5.3 represents the liquid fraction of deionized water in main discharge region at interval of 50µs with input parameters as mentioned above.

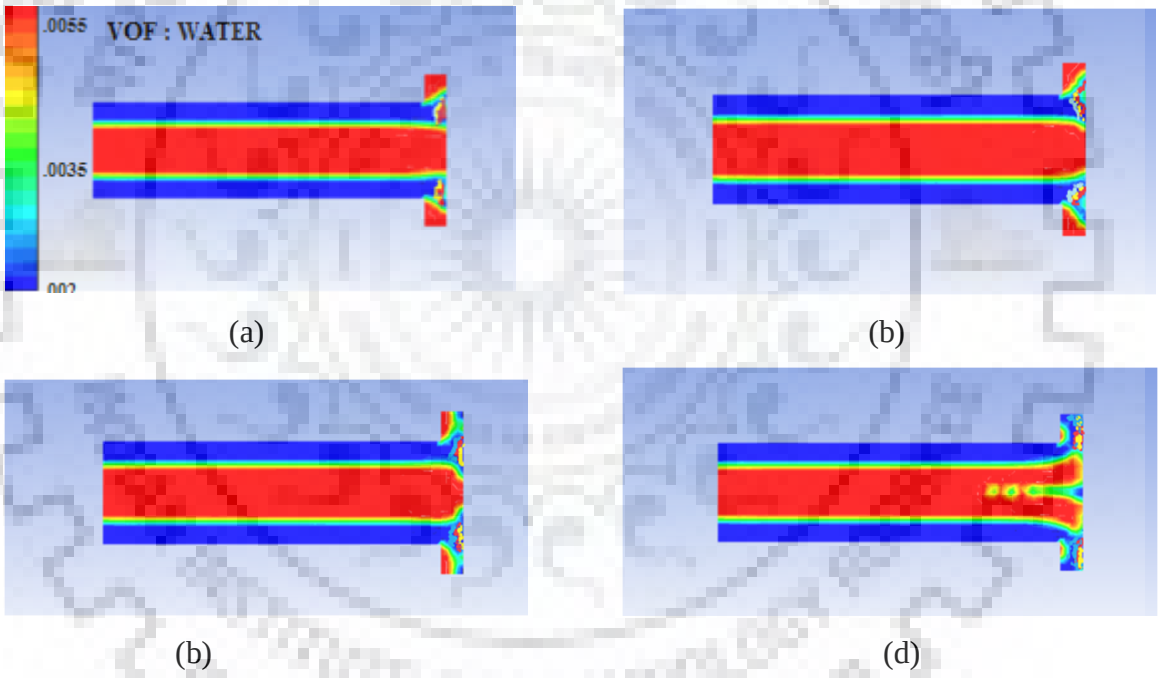

Figure 31 VOF simulation results at (a) 50 µs (b) 100µs (c) 150µs (d) 200µs for tool with helical flutes

The simulation results shows that Volume fraction of liquid dielectric in main discharge region varies between .0025-.0055. Which show that flow condition in this region results in high presence of liquid fraction thus higher dielectric strength in main discharge region which will ultimately increase the intensity of discharge energy and thus result in higher MRR. This is the reason why maximum MRR was experimentally observed in this combination of input parameters. Fuzuki at

al [7] similarly analysed the volume fraction of mist and our finding concur with their experimentation where MRR increased and dielectric strength increased where there was more fraction of liquid dielectric at main discharge region. Their finding that MRR is directly proportional to fraction of liquid dielectric concurs with our finding.

From our observation for optimum parameters the following section discusses the VOF model with parameters that gave minimum TWR i.e. cases where debris reattachment to tool was minimum. Initial conditions at pressure 25psi, liquid flow rate 9ml/min, tool with peripheral slots. Figure 5.4 represents the liquid fraction of deionized water in main discharge region at interval of 50µs with input parameters as mentioned above.

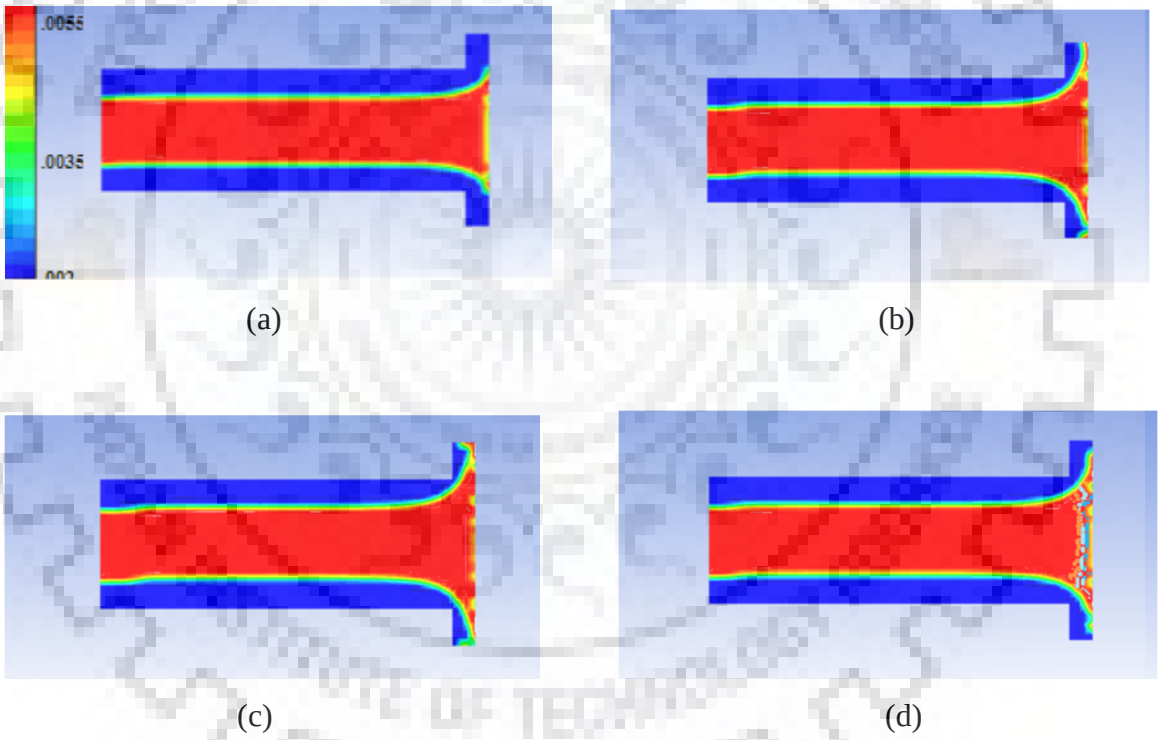

Figure 32 VOF simulation results at (a) 50 µs (b) 100µs (c) 150µs (d) 200µs for tool with tool having peripheral slots

Which show that volume fraction of water varies from .002-.0025 between the wall of tool and workpiece. This simulation results show that there will be least presence of liquid fraction hence weaker dielectric strength in this area and very miniscule chances of side spark are available. This

is the reason why minimum overcut was experimentally observed in this combination of input parameters.

CHAPTER 6

CONCLUSIONS AND FUTURE SCOPE

6.1 Conclusions

The following conclusions are drawn based on the experiments and the simulation conducted:

1. Simulation of mist flow, predicted the velocity of mist in IEG and its vicinity and showed that higher velocity of mist can be obtained by altering the geometry of tool. Also fraction of liquid dielectric can be controlled and regulated by making some vital changes, like helical flutes and peripheral slots, in tool geometry.
2. Experimentation results revealed that tool geometry plays the most critical role in machining, in terms of its contribution to machining outputs. Amongst all tool geometries, tool with helical flutes facilitated the effective flushing of IEG, thereby improving the MRR. Tool with peripheral slots was effective while machining shallow holes but once the tool moved deeper into hole the passage provided for debris removal, in form of peripheral slots, chocked by getting surrounded by inner walls of drilled holes and hence MRR reduced.
3. Debris reattachment to tool was effectively reduced by using pressure as high as 75 psi and liquid flow rate 9ml/min along with tools having passage for debris exit.
4. Pressure regulation is another critical factor when it comes to minimize hole over cut. Tool with helical flutes gave more time for debris interaction with inner walls of hole at the time when debris glided on flutes surface, which resulted in miniscule side sparks and hence hole over cut increased.

6.2 Future Scope

In the present study, near dry EDM was simulated on the basis of flow behaviour near main discharge regions which, by and large, controls the flushing conditions in the process and also directly or indirectly controls outputs like MRR, TWR and overcut. In future, it is possible to work with diverse geometrical changes in the tool and reduced number of assumptions to bring results that are far more close to reality. Also effects of temperature changes that come to due dielectric

breakdown and other electrical conditions can be brought in tandem with flow simulation. Magnetic field assistance in tandem with tool geometry variation can also be employed in future to further enhance the flushing condition in main discharge region to improve the quality characteristic of the machining process.

REFERENCES

1. NASA, Inert-gas electrical-discharge machining. NASA Technical Brief No. NPO15660(1985).

2 T. Tanimura, K. Isuzugawa, I. Fujita, A. Iwamoto, T. Kamitani, Development of EDM in the mist. in Proceedings of Ninth International Symposium of Electro Machining (ISEM IX) (Nagoya, Japan, 1989), pp. 313–316

3. X. Bai, Q. H. Zhang, T. Y. Yang, and J. H. Zhang, "Research on material removal rate of powder mixed near dry electrical discharge machining," *Int. J. Adv. Manuf. Technol.*, vol. 68, no. 5–8, pp. 1757–1766, 2013.

4. M. Kunieda, M. Yoshida, N. Taniguchi, ―Electrical Discharge Machining in Gas‖, Annals of the CIRP, (1997), Vol. 46, No.1, pp. 143-146

5. K . Dhakar, A. Dvivedi, and A. Dhiman, "Experimental investigation on effects of dielectric mediums in near-dry electric discharge machining," *J. Mech. Sci. Technol.*, vol. 30, no. 5, pp. 2179–2185, 2016.

6. G. Puthumana and S. S. Joshi, "Investigations into performance of dry EDM using slotted electrodes," *Int. J. Precis. Eng. Manuf.*, vol. 12, no. 6, pp. 957–963, 2011.

7. M. Fujiki, J. Ni, and A. J. Shih, "Investigation of the effects of electrode orientation and fluid flow rate in near-dry EDM milling," *Int. J. Mach. Tools Manuf.*, vol. 49, no. 10, pp. 749–758, 2009.

8. K. Wang, Q. Zhang, G. Zhu, and J. Zhang, "Effects of tool electrode size on surface characteristics in micro-EDM," *Int. J. Adv. Manuf. Technol.*, vol. 96, no. 9–12, pp. 3909–3916, 2018.

9. K. Wang, Q. Zhang, G. Zhu, Q. Liu, and Y. Huang, "Experimental study on micro electrical discharge machining with helical electrode," *Int. J. Adv. Manuf. Technol.*, vol. 93, no. 5–8, pp. 2639–2645, 2017.

10. M. Bhaumik and K. Maity, "Effect of Electrode Materials on Different EDM Aspects of

Titanium Alloy," *Silicon*, vol. 11, no. 1, pp. 187–196, 2019.

11. E. Oezkaya, N. Beer, and D. Biermann, "Experimental studies and CFD simulation of the internal cooling conditions when drilling Inconel 718," *Int. J. Mach. Tools Manuf.*, vol. 108, pp. 52–65, 2016.

12. A. Gholipoor, H. Baseri, M. Shakeri, and M. Shabgard, "Investigation of the effects of magnetic field on near-dry electrical discharge machining performance," *Proc. Inst. Mech. Eng. Part B J. Eng. Manuf.*, vol. 230, no. 4, pp. 744–751, 2016.

13. J. Tao, J. Ni, and A. J. Shih, "Modeling of the Anode Crater Formation in Electrical Discharge Machining," *J. Manuf. Sci. Eng.*, vol. 134, no. 1, p. 011002, 2012.

14. S. A. Mullya and G. Karthikeyan, "Accretion behavior and debris flow along interelectrode gap in μ ED-milling process," *Int. J. Adv. Manuf. Technol.*, vol. 96, no. 9–12, pp. 4381–4392, 2018.

15. B. Xie, Y. Zhang, J. Zhang, S. Ren, and X. Liu, "Flow Field Simulation of Ultrasonic Vibration Assisted EDM of Holes Array," *Proc. - 2015 7th Int. Conf. Adv. Commun. Networking, ACN 2015*, pp. 28–31, 2016.

16. M. Fujiki, J. Ni, and A. J. Shih, "Tool Path Planning for Near-Dry EDM Milling With Lead Angle on Curved Surfaces," *J. Manuf. Sci. Eng.*, vol. 133, no. 5, p. 051005, 2011.

17. X. Bai, Q. H. Zhang, T. T. Li, and J. H. Zhang, "Powder Mixed near Dry Electrical Discharge Machining," *Adv. Mater. Res.*, vol. 500, pp. 253–258, 2012.

18. S. Wang, "Applications of process engineering principles in materials processing, energy and environmental technologies—contributions of Professor Ramana Reddy," *Miner. Met. Mater. Ser.*, vol. 22, no. 9783319510903, pp. 3–14, 2017.

19. V. A. Alves, C. M. A. Brett, and A. Cavaleiro, "Influence of heat treatment on the corrosion of high speed steel," *J. Appl. Electrochem.*, vol. 31, no. 1, pp. 65–72, 2001.

20. Dvivedi A., Kumar P., "Surface quality evaluation in ultrasonic drilling through the Taguchi technique," Int. J. Adv. Manuf. Technol. (2007) 34:131-140, 2006.